

Hard-Substrate Reconnaissance
Survey S9404
Final Analysis Report

Massachusetts Water Resources Authority

Environmental Quality Department
Technical Report Series No. 95-1



**HARD-SUBSTRATE RECONNAISSANCE SURVEY S9404
FINAL ANALYSIS REPORT**

FOR

MWRA HARBOR AND OUTFALL MONITORING PROJECT

Submitted to

**MASSACHUSETTS WATER RESOURCES AUTHORITY
ENVIRONMENTAL QUALITY DEPARTMENT
100 FIRST AVENUE
CHARLESTOWN NAVY YARD
BOSTON, MA 02129
(617) 242-6000**

Prepared by

**DOUGLAS A. COATS
EIJI IMAMURA
JAMES F. CAMPBELL**

**MARINE RESEARCH SPECIALISTS
3639 EAST HARBOR BOULEVARD, SUITE 208
VENTURA, CA 93001-4277
(805) 644-1180**

MARCH 1995

ENVIRONMENTAL QUALITY DEPARTMENT TECHNICAL REPORT SERIES 95-1

Note: Figure 12 (Pages 28 and 29) was originally contained on two 11" * 17" foldout pages. High costs for the incorporation of foldout pages into the report led to it being reformatted into four 8.5" * 11" pages, 28(a&b), and 29 (a&b). Unbound copies of the figure in its original format are available from the authority upon request.

Citation:

Coats, D.A., E. Imamura, and J.F. Campbell. 1995. Hard-Substrate Reconnaissance Survey S9404 Final Analysis Report. MWRA Enviro. Quality Dept. Tech. Rpt. Series No. 95-1. Massachusetts Water Resources Authority, Boston, MA. 48 pp.

TABLE OF CONTENTS

LIST OF FIGURES	ii
LIST OF TABLES	iv
SUMMARY	1
1.0 INTRODUCTION	2
1.1 BACKGROUND AND OBJECTIVES	2
1.2 CRITERIA FOR SELECTING MONITORING LOCATIONS	5
2.0 METHODS	7
2.1 FIELD SURVEY	7
2.2 SAMPLE ANALYSIS	7
2.3 MEGAFUNAL ANALYSES	8
3.0 RESULTS	12
3.1 MEGAFUNAL COMMUNITY	12
3.1.1 Comparison with Other Regional Studies	12
3.1.2 Relationship Among Taxa	12
3.2 MEGAFUNAL AND TEXTURAL DISTRIBUTIONS	13
3.2.1 Water Depth	13
3.2.2 Relief Height	15
3.2.3 Geographic Distribution	27
4.0 RECOMMENDATIONS	31
4.1 HARD-SUBSTRATE SITES	31
4.2 NEAR-FIELD SEDIMENTARY SITES	31
5.0 LITERATURE CITED	39

LIST OF FIGURES

Figure 1	Location of target transects superimposed on topography determined by Bothner et al. (1992). Also shown is the location of the benthic infaunal station s4. Inset shows the study-area location within Massachusetts Bay.	3
Figure 2	Post-survey location of transects. Heavy lines reflect the actual course of the ROV and light lines are target transects from Figure 1	4
Figure 3	Dendrogram resulting from clustering (group average sorting) of Bray-Curtis similarity among the 26 taxa that were present in more than three transect subsections	14
Figure 4	Depth distribution of selected taxa having a negative correlation with water depth. Correlation coefficients from Table 3 are shown in brackets	17
Figure 5	Depth distribution of selected taxa having a positive correlation with water depth. Correlation coefficients from Table 3 are shown in brackets	18
Figure 6	Variation in depth, substrate size and the abundance of six selected taxa along Transect T1	21
Figure 7	Variation in depth, substrate size and the abundance of six selected taxa along Transect T2	22
Figure 8	Variation in depth, substrate size and the abundance of six selected taxa along Transect T3	23
Figure 9	Variation in depth, substrate size and the abundance of six selected taxa along Transect T4	24
Figure 10	Variation in depth, substrate size and the abundance of six selected taxa along Transect T5	25
Figure 11	Variation in depth, substrate size and the abundance of six selected taxa along Transect T6	26
Figure 12	Dendrogram resulting from clustering (group average sorting) of Bray-Curtis similarity among transect subsections	28
Figure 13	Location of shallow high-relief sites listed in Table 5. Numbers with a "T" prefix refer to transects and the "S" prefix indicates subsections	33
Figure 14	Location of shallow low-relief sites listed in Table 5. Numbers with a "T" prefix refer to transects and the "S" prefix indicates subsections	34
Figure 15	Location of deep low-relief sites listed in Table 5. Numbers with a "T" prefix refer to transects and the "S" prefix indicates subsections	35

Figure 16 Location of deep high-relief sites listed in Table 5. Numbers with a "T" prefix refer to transects and the "S" prefix indicates subsections. 36

Figure 17 Location of deep sediment sites and the benthic infaunal sampling stations s4 and NF19. Numbers with a "T" prefix refer to transects and the "S" prefix indicates subsections 37

LIST OF TABLES

Table 1	Categories used to characterize the hard-substrate features encountered along transect subsections	8
Table 2	Taxa identified in color video images listed by the relative accuracy of enumerations. Also shown is the taxon's rank by total abundance over all transects	9
Table 3	Pearson correlation coefficients between logarithmically-transformed taxon abundance and water depth. Shaded coefficients are not statistically significant at the 95% confidence level	16
Table 4	Pearson correlation coefficients between logarithmically-transformed taxon abundance and substrate size. Shaded coefficients are not statistically significant at the 95% confidence level	20
Table 5	Recommended hard-substrate sampling locations	32
Table 6	Location of deep sedimentary deposits	38

SUMMARY

Over eight hours of color video and 186 still photographs were collected along 9 km of seafloor near an outfall diffuser within Massachusetts Bay. Transects were divided into 50-m subsections along which benthopelagic megafauna were enumerated and bottom conditions digitized. The survey was conducted for reconnaissance of monitoring sites to be used in assessing potential anthropogenic effects from future wastewater discharge. Sites suitable for hard-substrate sampling were selected based upon proximity to the diffuser, continuity of megafaunal distributions, and four combinations of water depth and substrate relief height. The highest megafaunal similarities occurred between adjacent subsections which traversed seafloor areas of similar water depth and substrate height. Shallow high-relief sites were most common with five regions suitable for hard-substrate monitoring. These five regions covered over 3 km of seafloor at water depths shallower than 30 m and at distances ranging between 290 m and 1200 m from the diffuser. The three regions recommended for monitoring of shallow low-relief epifauna covered nearly 1.4 km of seafloor at distances ranging between 300 m and 1,400 m from the diffuser. Because of the geomorphology of the region, deep (>30 m) hard-substrate sites were less common, particularly for high-relief features (*viz.*, those extending beyond 1 m above the seafloor). The four regions characteristic of deep low-relief megafauna span a total distance of over 2 km and range between 64 m and 868 m from the diffuser. Four regions deemed suitable for sampling of deep high-relief epifauna covered only 334 m of seafloor and included one of the diffuser caps. Thus, distance from the diffuser-cap corridor ranged between 0 m and 217 m for deep high-relief sites.

1.0 INTRODUCTION

1.1 BACKGROUND AND OBJECTIVES

This report summarizes the results of a hard-substrate benthic reconnaissance survey (Imamura, 1994) conducted within Massachusetts Bay using a remotely operated vehicle (ROV). The survey is part of an ongoing effort to characterize the marine environment around the diffuser-cap corridor at the terminus of the outfall recently constructed for the Massachusetts Water Resources Authority (Figure 1). Wastewater discharge is expected to begin in May 1996 and studies conducted to date provide baseline pre-discharge data which will be used to assess future impacts of the outfall. The reconnaissance survey was intended to provide a "semi-quantitative" census of seafloor features and associated megafauna. This census was to be used to select future monitoring sites where fully-quantitative investigations could be conducted. The fully-quantitative field sampling would be designed such that statistical hypotheses concerning potential anthropogenic effects could be rigorously tested.

Six transects were traversed during the reconnaissance survey. The location of the six transects were selected to survey faunal distribution along the tops of drumlins and along depositional lows within 2 km of the diffuser-cap corridor. Figure 1 shows the location of the study area along with target transects. Data collected along the transects consists of continuous color video images and opportunistic still photographs of benthic epifauna. Extensive analysis of these images established a database that documents the distribution of bottom type and large benthopelagic organisms within 2 km of the diffuser-cap corridor (Coats and Campbell, 1994). Organisms of identifiable size (≥ 5 cm) or color contrast were enumerated from an examination of over eight hours of color video images collected along the six transects. Post-survey navigational locations of the ROV are superimposed on target transects in Figure 2. Lateral excursions from target transects were minimal and generally less than 100 m. To quantify local variability in substrate and epifauna, transects were divided into subsections with a 50-m nominal length. Occasionally, subsections were prematurely shortened due to ROV entanglement in lobster-trap lines and subsequent surfacing. This results in the discontinuities between subsections shown in Figure 2. The length of the remaining subsections ranged from 30 to 84 m. In addition to biological enumeration, the character of the substrate was categorized along each subsection.

In this report, the resulting census and bottom-type data are used to select hard-substrate sites for future monitoring of potential effects from outfall discharge on the local epifaunal community. Presently, monitoring of the benthic biological community is conducted only at sedimentary sites surrounding the diffuser-cap corridor (*e.g.*, Coats *et al.*, 1995). Addition of hard-substrate monitoring sites will supplement existing soft-bottom monitoring of benthic fauna in several ways. First, existing sedimentary sites are mostly located to west of the diffuser because of the paucity of soft-substrate regions to the east suitable for grab sampling. Addition of hard-substrate monitoring locations to the east of the diffuser-cap corridor would provide a more radially-symmetric sampling design. However, given the comparatively weak residual circulation in the region, it is unlikely that the existing soft-substrate sampling locations would miss significant impacts due to preferential advection of the outfall discharge to the west.

Another enhancement offered by a hard-substrate sampling is an expanded depth range. Soft-bottom sampling sites tend to be located in topographic lows where accumulation of sediment is sufficient for grab sampling. Consequently, the depth range of nearfield soft-bottom sites does not reflect the actual range in local bathymetry. Because of the comparative lack of depth variability, the relationship between nearfield infaunal distribution and depth was found to be weak compared to that of far-field infaunal stations, which traverse a wider range in depths over broad areas in Massachusetts and Cape Cod Bays (Coats *et al.*, 1995). As will be shown in this report, many benthopelagic macrofaunal taxa within 2 km of the diffuser-cap corridor also exhibit a significant depth-related distribution. The addition of hard-substrate sampling sites atop nearfield moraines would allow assessment of potential anthropogenic effects on taxa endemic to water depths shallower than the depositional lows sampled by nearfield infaunal stations. In addition to depth differences, hard-substrate monitoring sites

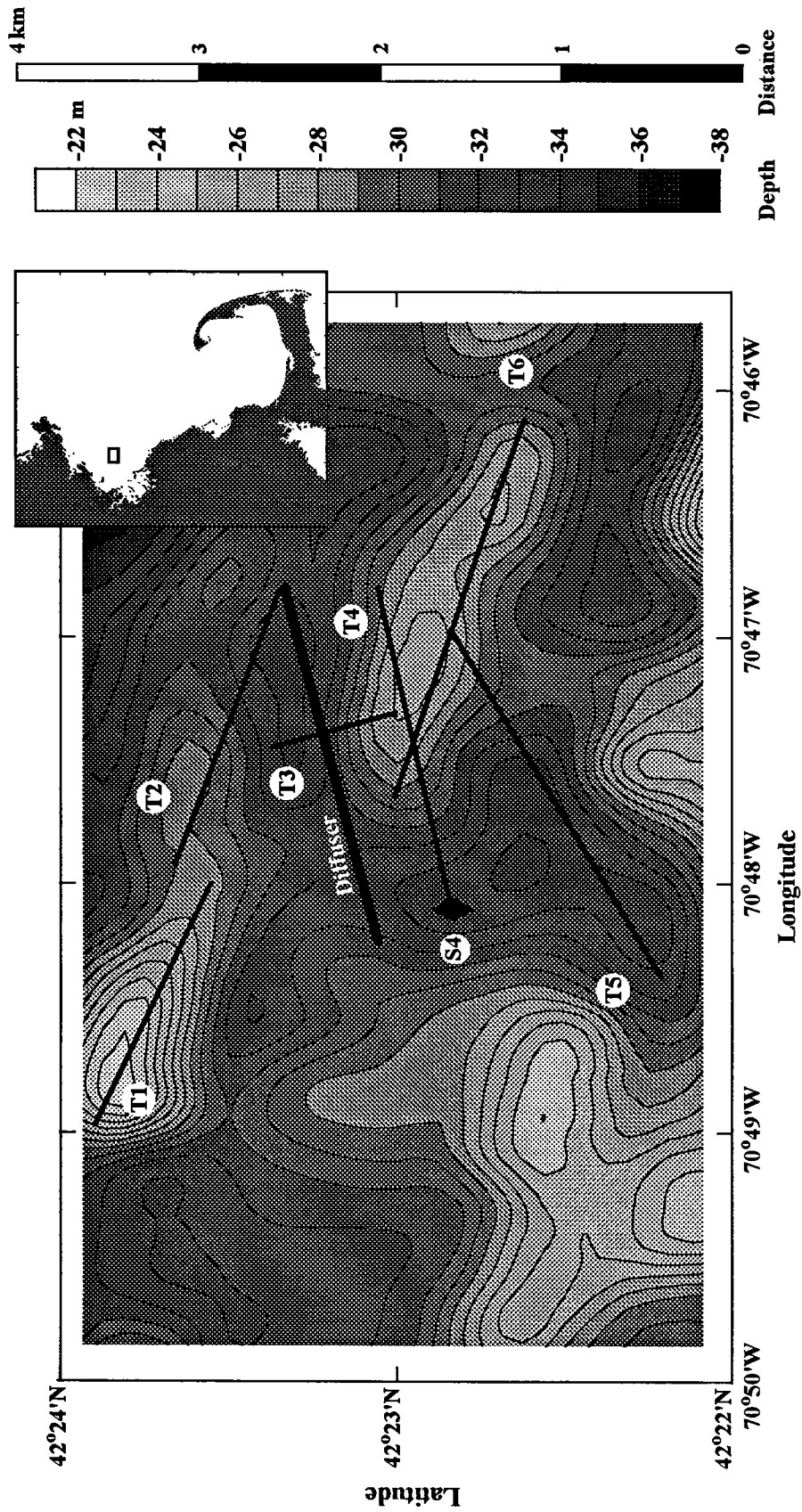


Figure 1. Location of target transects superimposed on topography determined by Bothner et al. (1992). Also shown is the location of the benthic infaunal Station S4. Inset shows the study-area location within Massachusetts Bay.

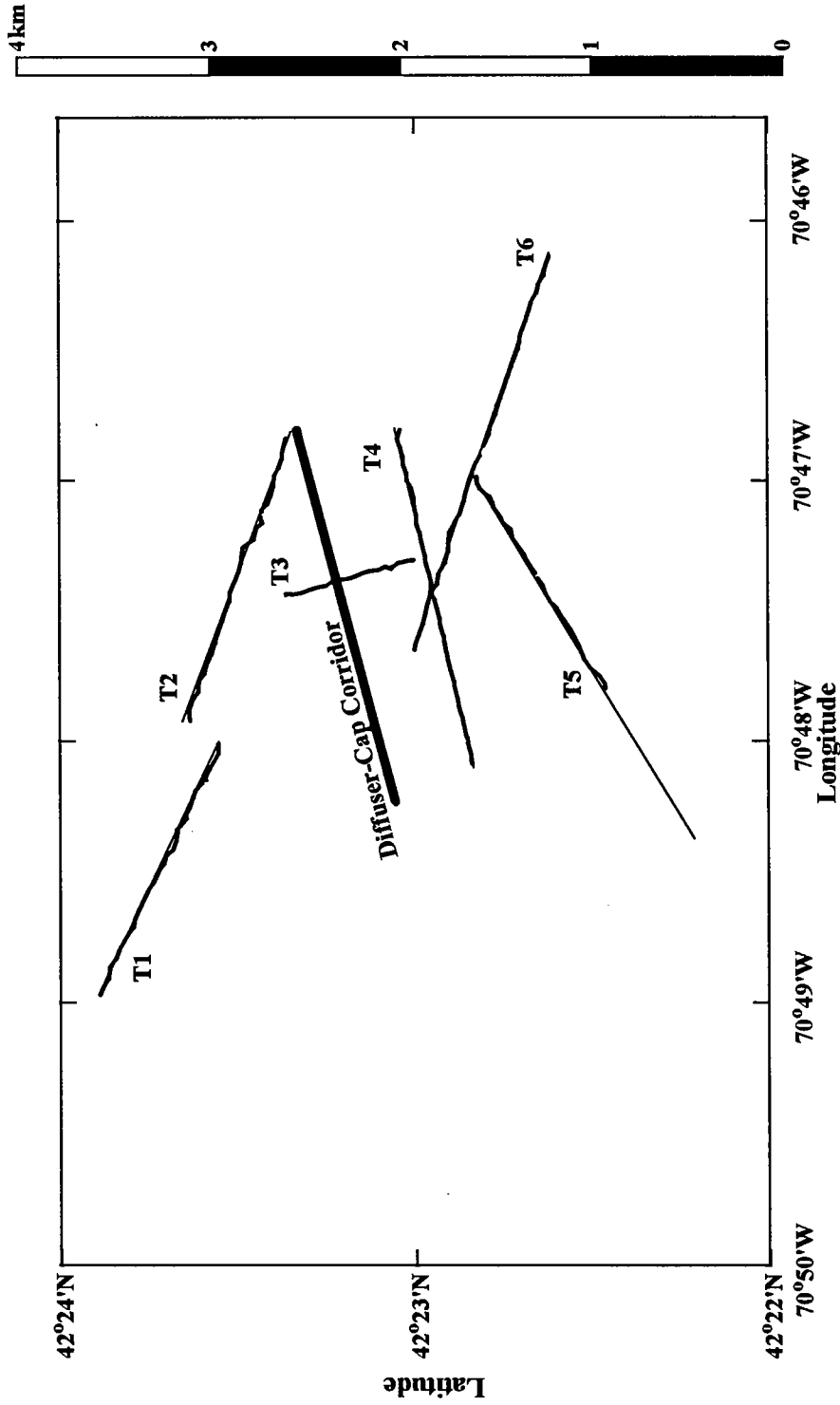


Figure 2. Post-survey location of transects. Heavy lines reflect the actual course of the ROV and light lines are target transects from Figure 1.

could increase anthropogenic detectability because of faunal differences between hard and soft-substrate communities were fully quantitative studies to be pursued. The hard-substrate epifauna observed in this survey include organisms, such as anemones, related to those found to be sensitive to increased particulate loads offshore California (Hyland *et al.*, 1994). In any regard, hard-substrate epifauna could react differently to sewage effluent exposure and their inclusion is likely to enhance the overall monitoring effort.

A second, ancillary objective of this report is identification of additional sedimentary sites near the diffuser corridor that could augment the benthic infaunal sampling array used in prior years (Blake *et al.*, 1993; Coats *et al.*, 1995). For example, a new sedimentary site close to the diffuser, designated Station S4, was successfully sampled for benthic infauna and sediment chemistry with a grab sampler in 1994 (Campbell, 1994). Station S4 is located 450 m off the southwest end of the diffuser-cap corridor, near the end of Transect T4 (Figure 1). Because it is a new soft-bottom sampling location, the long-term stability of its sediments and their lateral extent is of interest for continued monitoring. Some discussion on the character of this and other depositional regions is included in Section 4.2.

Because the survey was only intended for reconnaissance purposes, the resulting database used herein, does not provide a fully-quantitative baseline characterization of hard-substrate communities suitable for detecting future effects of effluent discharge. This is due to a number of limitations in the database. First, there was no *a priori* attempt at replication. Also, video imagery was of limited resolution and the resulting enumeration undoubtedly underestimates the abundance of smaller benthopelagic species (Uzmann *et al.*, 1977). Finally, the image area was not precisely determined as part of the reconnaissance survey. The distance of the ROV from the bottom ranged between 1 and 3 m, and image size was generally consistent within the survey. While this was adequate for site reconnaissance, fully quantitative baseline characterization of hard-substrate biological communities requires more rigorous sampling protocols. For example, replicated still photographs of known lateral dimension and quality sufficient to fully identify megafaunal organisms would permit quantitative enumeration using techniques described by Foster *et al.* (1991). Knowledge of the photoquadrat size is crucial for precise quantification of areal abundance estimates. Thus, while the abundance database may not be acceptable for comparison with other studies, or as baseline data for detecting anthropogenic effects, it is suitable for contrasting the epifaunal community along the different sections of transects covered by the reconnaissance survey.

1.2 CRITERIA FOR SELECTING MONITORING LOCATIONS

Three criteria will be used for selecting candidate hard-substrate monitoring sites. First, the character of the hard substrate, specifically the lateral extent, density and size of rocks and boulders, will be compared among candidate sites. Quantitative sampling, for example using photoquadrat techniques, requires the presence of many suitable sampling locations for replication, namely, numerous rock surfaces in close proximity that have dimensions comparable to or exceeding the camera's field of view. A second criterion pertains to the biological community structure at the candidate sampling site. As will be shown in this report, the distribution of certain taxa is dictated by water depth and substrate size (*e.g.*, high-relief versus low relief). Lastly, the third criterion is proximity to the diffuser. Testing statistical hypotheses for anthropogenic effects will depend on a comparison of similar sites both close to the effluent discharge (treatment sites) and remote from effluent effects (control sites).

Most of the analyses reported here address the second criterion relating to the distribution of megafaunal organisms. Future studies conducted to detect change in the hard-substrate epifauna will require an analysis of variance on photoquadrat data with several treatment conditions (*e.g.*, deep versus shallow, nearfield versus farfield, high-relief versus low-relief). An adequate statistical sample for detection of anthropogenic change in deep benthic communities requires a large number of replicate photoquadrats, nominally 60 (Hyland *et al.*, 1994) to 80 (Hardin *et al.*, 1993), from sampling sites of similar character. In shallower areas, the higher faunal density may allow far fewer replicates, such as the 12 replicates used for rocky subtidal communities in Massachusetts

Bay (Witman and Sebens, 1993). Collection of an adequate number of replicates at depth requires a region with uniform physical and biological characteristics over a spatial extent that is large compared to the photoquadrat size (nominally ≤ 1 m). To this end, similarity analysis of community structure, described in Sections 3.0, serves to identify regions where the benthic biology is relatively uniform. Specifically, groups of adjacent subsections with highly similar community structure are specified for sites with four different physical characteristics: i) shallow high-relief, ii) shallow low-relief, iii) deep low-relief and iv) deep high-relief. Section 2.0 describes the methodology used to analyze the benthopelagic community structure. Finally, Section 4.0 recommends candidate sites on both hard and soft substrate, suitable for future monitoring efforts.

2.0 METHODS

2.1 FIELD SURVEY

The hard-substrate reconnaissance survey (S9404) was conducted on September 16 and 17, 1994 (Imamura, 1994). The M/V *Marlin* served as support-ship to a Phantom DS4 Remotely Operated Vehicle (ROV). Photosamples were collected using a high-resolution color video camera and a 35-mm still camera mounted on the ROV. Photosamples were gathered near the diffuser-cap corridor along six transects shown in Figure 1. Digital data pertaining to the ROV depth, heading and position as well as transect number and time were overlaid on video images. These data were digitized (Coats and Campbell, 1994) and form the basis of the analyses described in this report.

2.2 SAMPLE ANALYSIS

A variety of techniques have been developed to quantify macrofaunal species (generally fishes) using video images collected by ROV (*cf.*, Michalopoulos *et al.*, 1992). They are based on either counts per unit time or distance. This analysis uses strip transect techniques (*e.g.*, Auster *et al.*, 1991) based on distance covered. Species-time techniques are problematic because the ROV speed varied substantially over the reconnaissance survey. Also, precise (≈ 1 m) navigation was available for distance computations and strip transect techniques produce spatially-based density estimates similar to those of infaunal monitoring studies.

Digitization and faunal enumeration of over 8 hours of color video and 186 still photographs were described in the data report for this survey (Coats and Campbell, 1994). Additionally, the character of the substrate was classified along each transect subsection as was the water depth and location. Substrate categories are listed in Table 1. Fauna was visually identified and enumerated from the video images along each transect subsection. Because of their inherently higher resolution, still photographs acted as visual voucher specimens and confirmed taxonomic identifications determined from video images. Two encrusting organisms, *Porifera* sp. A and a form of *Lithothamnium* spp., could not be counted individually and a percent cover was determined instead. The length of transect subsections varied for a number of reasons, including surfacing of the ROV due to entanglement or avoidance of lobster-trap lines. To compare the abundance of organisms in subsections of differing lengths, the number of organisms observed on the video was normalized by the length of the subsection. The resulting lineal densities (number of individuals m^{-1}) for the thirty-seven identified taxa were used in epifaunal analyses described below.

Table 1. Categories used to characterize the hard-substrate features encountered along transect subsections.

<u>Size Range: Diameter of the largest hard-substrate features</u>	
Category	Size Range
Absent	Little or no hard-substrate larger than 1-in diameter
Cobbles	1 in \leq diameter < 6 in
Rocks	6 in \leq diameter < 3 ft
Boulders	3 ft \leq diameter < 9 ft
Large Boulders	\leq 9 ft
Diffuser	Diffuser Cap (\leq 9 ft)

<u>Distribution: Skewness of the frequency distribution of hard-substrate features</u>	
Category	Size Distribution
Uniform	All features are nearly the same size
Skewed	Majority of features are of the largest size
Broad	Sizes are uniformly distributed

<u>Coverage: Amount of hard-substrate encountered along a transect subsection</u>	
Category	Coverage
Rare	0-25% hard-substrate cover
Scattered	26-50% hard-substrate cover
Dense	51-75% hard-substrate cover
Continuous	76-100% hard-substrate cover

<u>Veneer: Type of material, if any, covering hard substrate features</u>	
Category	Veneer
Bare	Majority of rock was exposed
Detritus	Thin veneer of detritus covered most rock surfaces
Hydroid	Hydrozoan turf covering rock
Sediment	Thick sediment

<u>Grain Size: Type of granular material surrounding hard substrate features</u>	
Category	Grain Size
Mud	Silt and Clay
Coarse	Sand and gravel

2.3 MEGAFUNAL ANALYSES

Data resulting from fully-quantitative photoquadrat analyses are biological abundance measures similar to those determined for infaunal organisms as part of the outfall monitoring program (*e.g.*, Coats *et al.*, 1995). Specifically, areal density of epifaunal organisms is computed by normalizing the number of organisms within a specific taxa by the area of hard-substrate observed within each photoquadrat. In a fully quantitative analysis, the quadrat size can be precisely determined from computations of coverage area of the still photograph. Ideally, image area can be determined from the focal length of the camera lens, its angular field-of-view, the camera's distance from the organism, and the angle of inclination of the viewing axis (Wakefield and Genin, 1987). However, organism density estimates are sensitive to the variability in image area and, over a rough

bottom, the requisite positioning and stability of the camera platform is often not practical. In some studies (e.g., Hecker, 1990), introduction of objects of known dimension (e.g., metric scales or grids) into images has provided coverage information suitable for projecting life-size images during identification and enumeration of megafauna. The use of comparatively unstable ROVs as camera platforms has prompted a more direct method for determining scale information. It is now common to use parallel lasers that produce small light spots of known separation on a video image or still image (Tusting and Davis, 1992; Davis and Pilskaln, 1992). Video images collected using an ROV are subject to its changes in altitude, pitch, and roll which results in a variable field of view along transects.

The data provided by the hard-substrate reconnaissance survey differs from quantitative still photoquadrat data in some other significant ways. First, since still photographs were not intended for quantitative analysis, they were collected in an opportunistic rather than random manner. For true replication, photoquadrats should be collected randomly. Instead, since the reconnaissance photographs were primarily for identification of organisms rather than enumeration, particularly clear images of representative biological specimens were sought. Furthermore, the image coverage area and the substrate type and orientation were of a lesser concern than image quality.

The color video images used in this study to quantify biological distributions, differ from fully quantitative photoquadrat surveys in another way. The strip transect analysis technique results in lineal rather than areal density estimates of organism abundance. Consequently, abundance determined in this study cannot be directly compared with that of infaunal investigations (e.g., Coats *et al.*, 1995 and Blake *et al.*, 1993). Although lineal density derived from video is only semi-quantitative compared to rigorously-conducted photoquadrat sampling, it has the advantage of rapidly characterizing large regions. This was the intent of this reconnaissance survey. Other limitations of the census database were due to variation in ROV speed over the seafloor, transit over a widely varying substrate within a single subsection, changes in video-camera angle relative to the seafloor and limited water clarity. Also, because of differences in the size and coloration of epifauna, the enumeration of certain taxa was more accurate and less sensitive to variations in the ROV sampling-platform than other taxa. Table 2 lists the thirty-seven identified taxa along with a qualitative assessment of the accuracy of the lineal density estimates. The epifaunal analyses described in this report, focus on those taxa whose enumeration was of moderate to high quality.

Table 2. Taxa identified in color video images listed by the relative accuracy of enumerations. Also shown is the taxon's rank by total abundance over all transects.

Taxon	Common Name	Accuracy	Rank
<i>Boltenia ovifera</i>	stalked tunicate	High	13
<i>Agarum cribrosum</i>	sea colander	High	8
<i>Cancer</i> spp.	crab	High	15
<i>Homarus americanus</i>	American lobster	High	14
<i>Pleuronectes americanus</i>	winter flounder	High	21
<i>Placopecten magellanicus</i>	deep sea scallop	High	21
<i>Cerianthus borealis</i>	northern cerianthid	High	23
<i>Asterias</i> spp.	sea star	High	10
<i>Henricia sanguinolenta</i>	blood sea star	High	9
<i>Haliclona oculata</i>	finger sponge	High	25
<i>Metridium senile</i>	frilled anemone	High	5
<i>Ciona intestinalis</i>	sea vase	Moderate	20
<i>Crossaster papposus</i>	spiny sunstar	Moderate	16
<i>Strongylocentrotus droebachiensis</i>	green sea urchin	Moderate	7

Taxon	Common Name	Accuracy	Rank
<i>Halichondria panicea</i>	crumb-of-bread sponge	Moderate	19
<i>Raja laevis</i>	barn-door skate	Moderate	31
<i>Gadus morhua</i>	Atlantic cod	Moderate	17
<i>Tautogolabrus adspersus</i>	cunner	Moderate	6
<i>Urophycis</i> spp.	hake	Moderate	28
<i>Myoxocephalus</i> spp.	sculpin	Moderate	22
<i>Raja erinacea</i>	little skate	Moderate	31
<i>Halocynthia pyriformis</i>	sea peach	Moderate	27
<i>Melanogrammus aeglefinus</i>	haddock	Moderate	31
<i>Macrozoarces americanus</i>	ocean pout	Moderate	30
<i>Porifera</i> sp. B.	leaf sponge	Moderate	26
<i>Henricia sanguinolenta</i> (juv)	juvenile blood sea star	Moderate	12
<i>Modiolus modiolus</i>	northern horse mussel	Low	3
<i>Balanus</i> spp.	barnacle	Low	4
<i>Clupea harengus</i>	Atlantic herring	Low	11
<i>Rhodymenia palmata</i>	dulse	Low	1
<i>Rhodymenia</i> sp A.	pinnate red algae	Low	2
<i>Hemitripteris americanus</i>	sea raven	Low	31
<i>Pagurus</i> spp.	hermit crab	Low	29
<i>Porifera</i> sp. A.	orange encrusting sponge	Low	a
<i>Lithothamnium</i> spp.	purple encrusting algae	Low	a
<i>Porifera</i> spp.	sponge	Low	18
<i>Psolus fabricii</i>	scarlet psolus	Low	30

^a Encrusting taxa were quantified by percent cover and were not ranked with density estimates.

Three analyses were performed on the megafaunal data. The most basic was bathymetric profile plots combined with substrate size and taxon abundance along transects. Bivariate correlation was another common analysis technique used herein. Cluster analysis was the most important method used since it identified similar macrofaunal community structures among the large (193) number of transect subsections. The similarity between pairs of subsections was determined from numerical classification based on the unweighted pair-group method (Sneath and Sokal, 1973). Results were expressed in the form of dendrograms where sample pairs were ordered into groups of increasingly greater similarity as measured by resemblance between the abundance for individual species (Boesch, 1977).

The Bray-Curtis similarity coefficient (B) (Clifford and Stephenson, 1975; Swartz, 1978) was used to classify abundance data into groups of similar transect subsections. The similarity coefficient ranges between 0 and 1. For pairs of transect subsections that have identical numbers of individuals for each taxon, the coefficient is 1.00. The similarity coefficient is 0.00 when all taxa present in one sample are completely absent in the other sample and vice-versa. The Bray-Curtis coefficient was computed as follows

$$B_{jk} = \frac{2 \sum_{i=1}^s \min(N_{ij}, N_{ik})}{\sum_{i=1}^s (N_{ij} + N_{ik})}$$

where: B_{jk} = similarity coefficient between sample j and sample k
 S = total number of species
 N_{ij} = number of individuals for species i in sample j .

When computing B , the abundance (N) was logarithmically transformed.

3.0 RESULTS

3.1 MEGAFAUNAL COMMUNITY

The biological analyses described here were performed on epifaunal and pelagic taxa with large physical dimensions. For the purposes of this report, these taxa are designated megafauna. As described above, resolution limitation of the color video images prevents full identification and quantification of all epifaunal organisms. In practice, most organisms with diameters exceeding about 5 cm were successfully enumerated. Some smaller taxa, with coloration or shape easily distinguished from the surrounding substrate, were also identified. One example is the white juvenile sea star, whose high-contrast allowed rapid enumeration of most individuals even as small as 1 cm.

3.1.1 Comparison with Other Regional Studies

Many macrofaunal organisms observed in this study were also found in other video surveys in the region. In an area immediately to the south of Cape Cod near 40° 50'N, 70° 55'W, eight of the ten taxa observed by Auster *et al.* (1991) are listed in Table 2. Missing taxa included the shrimp *Crangon septemspinosa* and *Dichelopandalus leptocerus* which were deemed too small to enumerate without bias in the reconnaissance survey. Another video survey was performed by Battelle Ocean Sciences Center (1987) along transects covering a 95-km² area immediately west of the reconnaissance survey area. Twenty-three of the 37 taxa identified in video images from the 1994 reconnaissance survey were also identified from ROV video tapes in the 1987 survey.

The absence of eight of the 12 taxa in the earlier survey can be explained in terms of their low abundance in the 1994 survey. Seven of the missing taxa, *Cerianthus borealis* (northern cerianthid anemone), *Ciona intestinalis* (sea vase), *Crossaster papposus* (spiny sunstar), *Psolus fabricii* (scarlet psolus), *Raja laevis* (barn-door skate), *Gadus morhua* (Atlantic cod), and *Melanogrammus aeglefinus* (haddock) were only observed rarely in the recent survey and ranked in the lower 20 in abundance (Table 2). Also, although the ranking (11) of *Clupea harengus* (Atlantic herring) was relatively high, it resulted from a single encounter with large school. Differences in the remaining four taxa are more difficult to explain. Three of the remaining four taxa are macroalgae and include *Rhodomenia palmata* (dulse), *Rhodomenia* sp.A (pinnate red algae), and *Agarum cribrorum* (sea colander). Their absence may be due to differences in taxonomic identification since high abundances of *Fucus* spp. and *Laminaria* spp. were observed at some stations in the earlier survey. These taxa are typically associated with littoral and subtidal habitats much shallower than those of the surveys (Taylor, 1967). Also, one species of *Laminaria*, *L. agardhii* (southern kelp) is very similar in appearance to *A. cribrorum* (sea colander). The remaining missing species was *Strongylocentrotus droebachiensis* (green sea urchin). Although it was not described in the video transects of the earlier survey, it was collected by diver and by the ROV manipulator arm at some stations.

3.1.2 Relationship Among Taxa

A total of 26 of the 37 taxa was included in the numerical classification. Excluded were eight taxa, *Macrozoarces americanus* (ocean pout), *Pagurus* spp. (hermit crab), *P. fabricii* (scarlet psolus), *Hemitripterus americanus* (sea raven), *C. harengus* (Atlantic herring), *Raja erinacea* (little skate), *M. aeglefinus* (haddock), and *R. laevis* (barn-door skate), whose abundance was probably under sampled since they were only observed in less than four of the 193 transect subsections. Also excluded were the two encrusting organisms, *Porifera* sp. A (orange encrusting sponge) and *Lithothamnium* spp. (purple encrusting algae), which were quantified by percent cover rather than lineal density. Finally, unidentified sponges were also excluded to avoid confusion with identifiable species of sponge.

Two major groups, designated Group A and Group B, were identified by (R mode) numerical classification among taxa (Figure 3). Using a Bray-Curtis similarity index of 0.2 as a decision rule, the dendrogram separates all but four taxa into these two groups. Group A is the largest group and contains 17 of the 26 taxa present. Group B is three times smaller and contains only five taxa. The four taxa unaffiliated with the two cluster groups were *Urophycis* spp. (hake), *Haliclona oculata* (finger sponge), *Porifera* sp. B. (leaf sponge), and *Halocynthia pyriformis* (sea peach). All had comparatively low abundances as indicated by rankings exceeding 24 (Table 2). The two sponge taxa showed some affinity for one another at a similarity of 0.17. For reasons to be discussed in Section 4.2, *Urophycis* spp. (hake) was found exclusively along five transect subsections that were within large areas of thick sediment. This effectively isolated them from most of the other taxa which were distributed in areas containing hard substrate.

The high affinity among some taxa in Group A, described by relatively high (>0.75) similarity indices, can also be explained by anecdotal observations. Not surprisingly, the highest Bray-Curtis similarity index was computed between the two red algae, *R. palmata* (dulse) and *Rhodymenia* sp. A. (pinnate red algae). These taxa were consistently observed together on hard-substrate, and with great abundance at the shallow depth (<30 m). The algae *A. cribrosum* (sea colander) is also closely associated ($B=0.56$) with these taxa. A less intuitive affinity occurred between the sessile anthozoan *Metridium senile* (frilled anemone) and free-swimming fish *Tautoglabrus adspersus* (cunner) at a similarity of 0.77. Both species exhibited substantially higher abundances near large boulders. This unique spatial distribution accounts for a high similarity index between these apparently unrelated organisms.

Another high similarity worthy of note, occurred between taxa within the *Asterias* (sea star) genus and *Henricia sanguinolenta* juv (juvenile blood sea star). Normally, one would expect the highest similarity between the adult and juvenile forms of *H. sanguinolenta*. However, the juvenile form of sea star observed in the video images was small, close to the resolution capabilities for enumeration. Although marginal, it was postulated that these small sea stars were *H. sanguinolenta*. Assuming that juvenile and adult sea stars of these two species have similar habitat preferences, numerical classification suggests that most of these organisms were in fact, members of the genus *Asterias* rather than *Henricia*.

3.2 MEGAFaUNAL AND TEXTURAL DISTRIBUTIONS

This section examines various physical factors that determine the distribution of megafauna in the hard-substrate region with 2 km of the diffuser cap corridor. A similar study of deep hard-substrate communities offshore California (Hardin *et al.*, 1994) has shown that water depth and habitat relief (vertical dimension of the hard-substrate) are primary influences on epifaunal distribution. Other studies (Hecker, 1990; Rowe and Menzies, 1969; Haedrich *et al.*, 1975) have established a clear relationship between species composition and depth along the U.S. Atlantic Coast. The intent here is to establish ranges in the physical factors across which the megafaunal community structure is comparatively uniform. Transect subsections representative of these physical factors will then be selected to serve as candidate sites for a future fully-quantitative hard-bottom studies. With a fully-quantitative investigation, possible impacts from effluent discharge can be tested with a multiple analysis of variance model that accounts for confounding influences from natural variability in the physical environment.

3.2.1 Water Depth

The discussion now returns to the two major groups of taxa defined by the numerical classification of Figure 3. Initial speculation based on anecdotal observations suggests that groups were separated by substrate type. Three of the five taxa within the smaller of these two groups (Group B), namely *C. borealis* (northern cerianthid anemone), *Pleuronectes americanus* (winter flounder), and *Placopecten magellanicus* (deep sea scallop), were

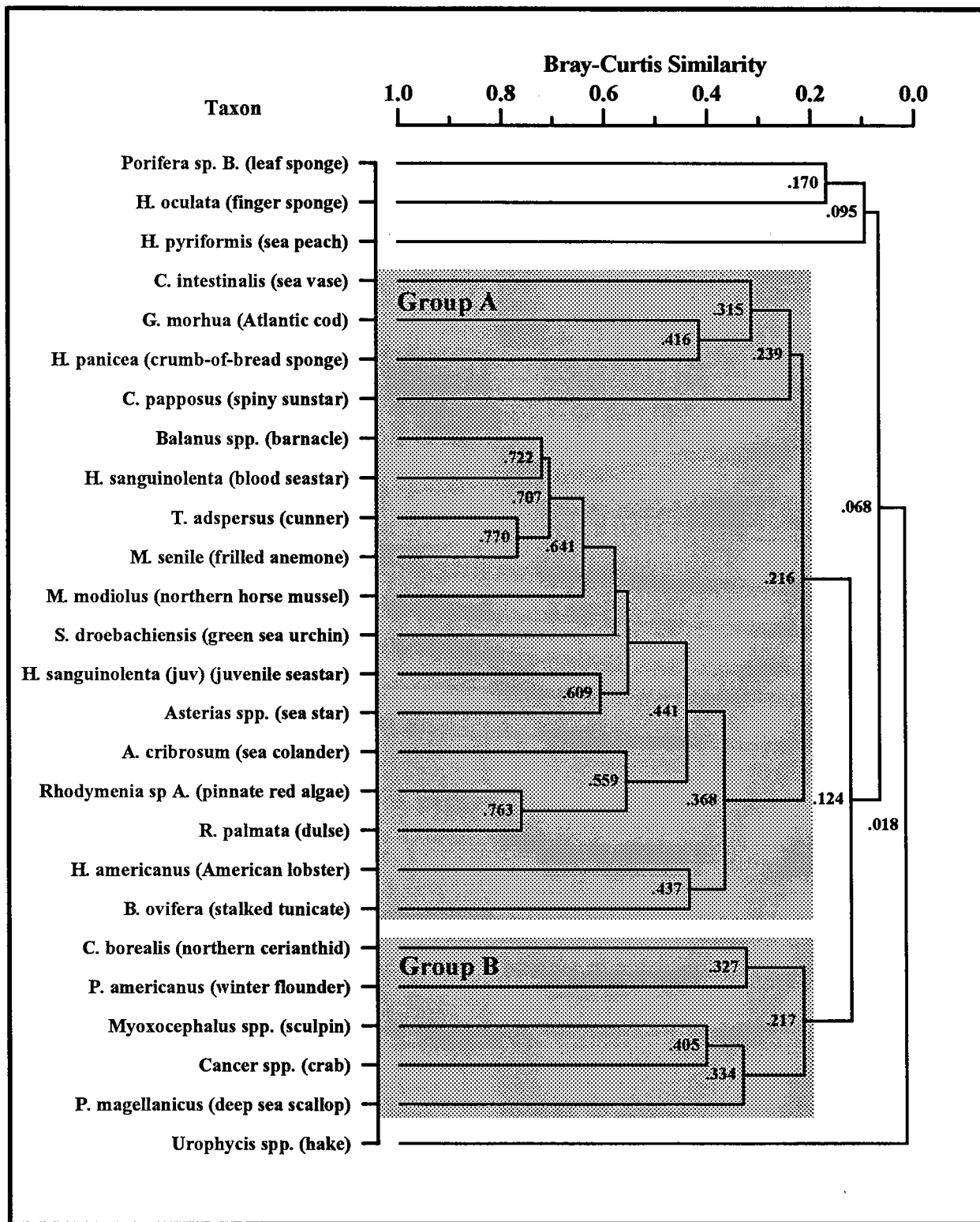


Figure 3. Dendrogram resulting from clustering (group average sorting) of Bray-Curtis similarity among the 26 taxa that were present in more than three transect subsections.

largely observed on sedimentary deposits rather than hard substrate. The 17 taxa in Group A were almost always associated with hard-substrate, although the highly motile organisms, *T. adspersus* (cunner), *G. morhua* (Atlantic cod), and *Homarus americanus* (American lobster), often ranged over sediment areas adjacent to hard-substrate features. From the foregoing discussion, substrate type appears to be an important influence on the distribution of taxa.

Anecdotal observations of a taxon's affinity for substrate type aside, a more quantitative analysis reveals that water depth and other related physical factors also serve to distinguish the two major cluster groups of Figure 3. Table 3 shows that the abundance of all five taxa in Group B was positively correlated with depth. Furthermore, their increased abundance at greater depth was statistically-significant at the 95% confidence level. In contrast, all but one of the 17 taxa in Group A were negatively correlated with water depth and eleven of these were statistically significant. *Asterias* spp. (sea star) was the sole positively-correlated taxon in Group A and its correlation was only marginally significant at the 95% confidence level.

Given that water depth was an important factor for megafaunal distribution, a single depth near 30 m was selected to partition "shallow" and "deep" regimes. Ideally, the transition depth would cleanly partition the abundance of all taxa by cluster group in Figure 3. In reality, each taxon differed in its distribution with depth and these differences cannot be determined from correlation coefficients alone. The Pearson correlations shown in Table 3 are predicated on a log-linear relationship between abundance and depth. While the abundance of some taxa varied monotonically with depth, others exhibited abrupt changes in abundance with depth. For example, the abundance of algae, shown in the bottom frame of Figure 4, declined abruptly below 28 m, and below 30 m, it was virtually absent. This is not surprising because macroalgae physiology requires sunlight for photosynthesis. Based on this information, the depth of the euphotic zone lies close to 30 m near the diffuser cap corridor.

In contrast to the depth distribution of macroalgae, tunicate abundance exhibited a nonlinear distribution as shown in the center frame of Figure 4. Although all had negative (linear) correlation coefficients, the abundance of *Boltenia ovifera* (stalked tunicate) reached a maximum near 28 m whereas the abundance of *C. intestinalis* (sea vase) was constant at depths less than 32 m. Other organisms in Group A of Figure 3, exhibited abundances that monotonically declined over the entire depth range as shown in the upper frame of Figure 4. A similar monotonic increase in abundance was evident in most of the positively-correlated taxa (Figure 5). Except for *Urophycis* spp. (hake), these taxa constitute Group B in Figure 3. Observations of *Urophycis* spp. were limited to depths below 32 m where large subsections containing deep sediments were found.

3.2.2 Relief Height

The vertical relief of hard-substrate features is another potential influence for epifaunal distribution. Unfortunately, the geomorphology of the study area made it difficult to separate the influence of water depth from relief height. This was because high-relief features (boulders) tended to be restricted to shallower depths. The Pearson correlation coefficient computed between water depth and substrate size was -0.49 over all transect subsections. The large negative correlation indicates a strong linear relationship between increasing water depth and decreasing substrate size. This relationship is not an artifact of the selected study area, but is instead, related to regional geology. The regional seafloor physiography consists of a series of elliptical drumlins with major axes oriented along 290°N (Figure 1). Two drumlins immediately adjacent to the diffuser-cap corridor were surveyed in this study. With a vertical relief of 10 m, they extend for 2 km along their major axis. An analysis of sonographs from the region by Knebel (1993) reveals erosional environments on the top of drumlins with deposition or reworking of fine-grained sediment at depth. Large boulders, some with diameters exceeding 3 m, were deposited along with other glacial till as part of the moraines. These boulder trains or erratics can be traced as strong acoustic reflectors in sub-bottom profiles as they extend under the sediments that fill

Table 3 . Pearson correlation coefficients between logarithmically-transformed taxon abundance and water depth. Shaded coefficients are not statistically significant at the 95% confidence level.

Taxon	Common Name	Depth Correlation
<i>Cerianthus borealis</i>	northern cerianthid	0.32
<i>Myoxocephalus</i> spp.	sculpin	0.28
<i>Cancer</i> spp.	crab	0.28
<i>Placopecten magellanicus</i>	deep sea scallop	0.28
<i>Pleuronectes americanus</i>	winter flounder	0.24
<i>Urophycis</i> spp.	hake	0.22
<i>Pagurus</i> spp.	hermit crab	0.18
<i>Asterias</i> spp.	sea star	0.16
<i>Raja erinacea</i>	little skate	0.11
<i>Raja laevis</i>	barn-door skate	0.11
<i>Macrozoarces americanus</i>	ocean pout	0.10
<i>Porifera</i> spp.	sponge	0.06
<i>Hemüripteris americanus</i>	sea raven	0.05
<i>Melanogrammus aeglefinus</i>	haddock	0.04
<i>Clupea harengus</i>	Atlantic herring	0.00
<i>Crossaster papposus</i>	spiny sunstar	-0.01
<i>Psolus fabricii</i>	scarlet psolus	-0.02
<i>Halictona oculata</i>	finger sponge	-0.02
<i>Porifera</i> sp. B.	leaf sponge	-0.03
<i>Henricia sanguinolenta</i> (juv)	blood sea star juvenile	-0.05
<i>Halichondria panicea</i>	crumb-of-bread sponge	-0.06
<i>Henricia sanguinolenta</i>	blood sea star	-0.06
<i>Gadus morhua</i>	Atlantic cod	-0.11
<i>Homarus americanus</i>	American lobster	-0.11
<i>Halocynthia pyriformis</i>	sea peach	-0.14
<i>Ciona intestinalis</i>	sea vase	-0.17
<i>Metridium senile</i>	frilled anemone	-0.19
<i>Boltenia ovifera</i>	stalked tunicate	-0.21
<i>Agarum cribrosum</i>	sea colander	-0.36
<i>Balanus</i> spp.	barnacle	-0.37
<i>Rhodymenia</i> sp A.	pinnate red algae	-0.38
<i>Modiolus modiolus</i>	northern horse mussel	-0.51
<i>Rhodymenia palmata</i>	dulse	-0.53
<i>Tautoglabrus adspersus</i>	cunner	-0.56
<i>Strongylocentrotus droebachiensis</i>	green sea urchin	-0.70

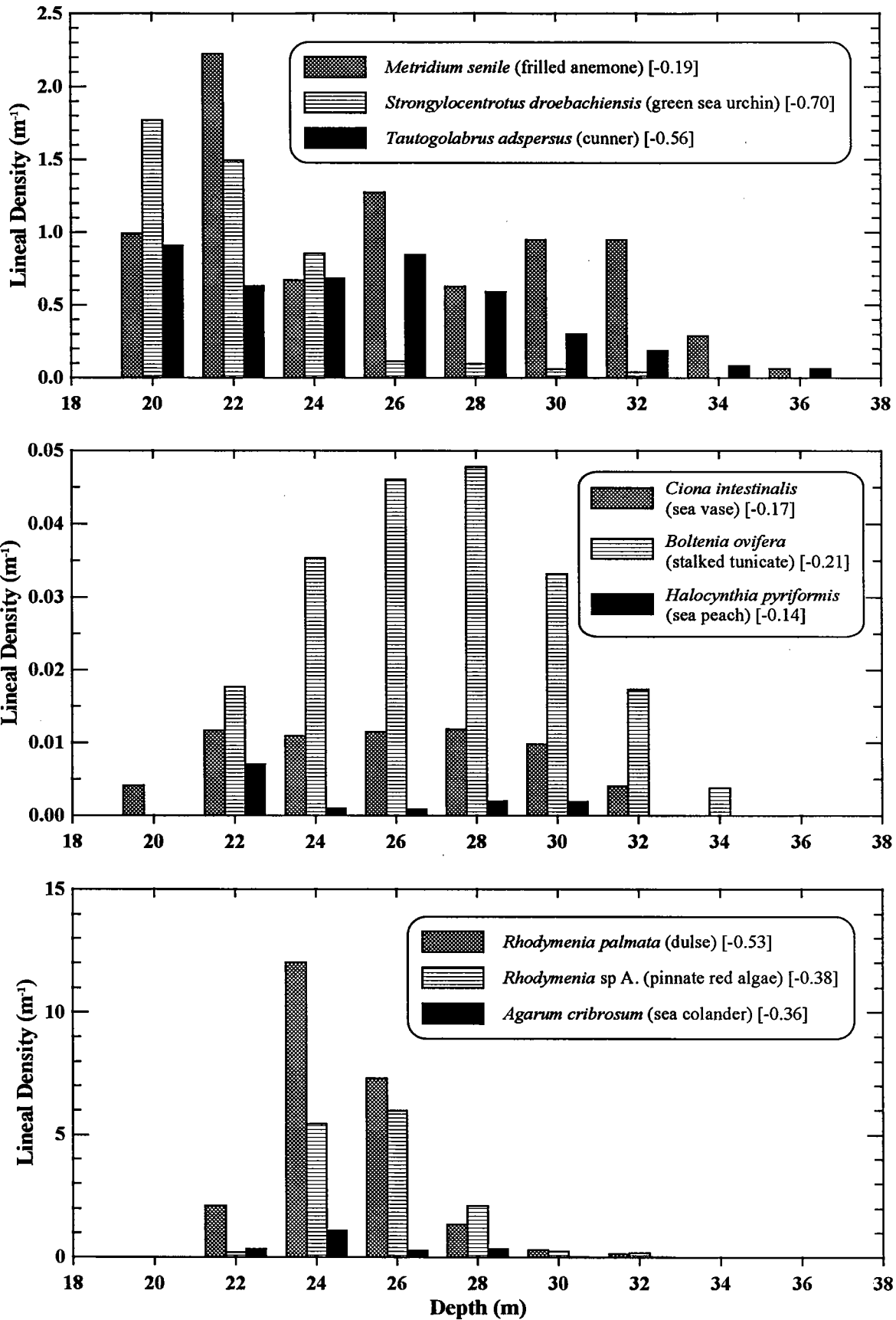


Figure 4. Depth distribution of selected taxa having a negative correlation with water depth. Correlation coefficients from Table 3 are shown in brackets.

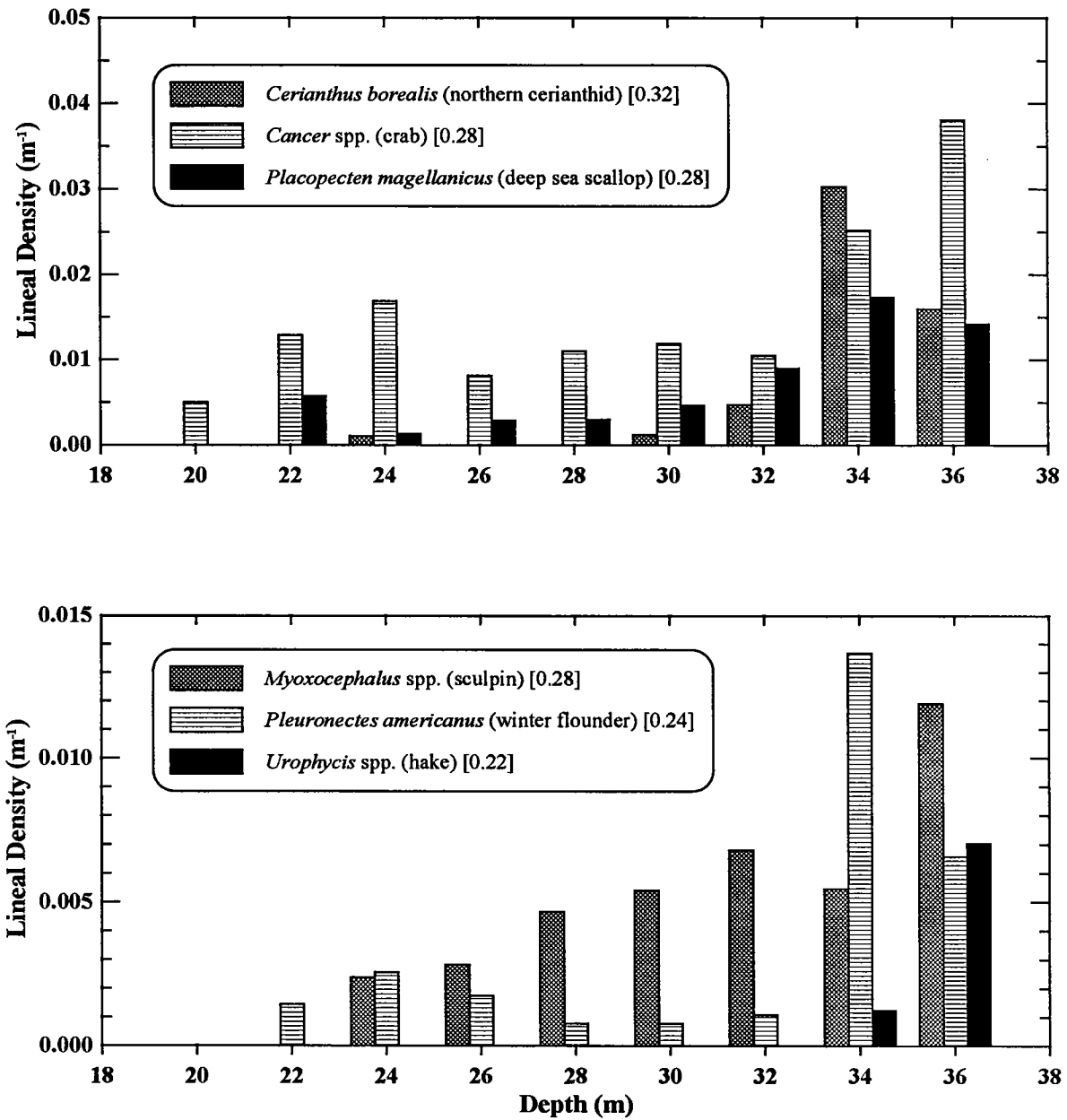


Figure 5. Depth distribution of selected taxa having a positive correlation with water depth. Correlation coefficients from Table 3 are shown in brackets.

adjacent depressions. Thus, large hard-substrate features are not absent at depth, but are buried and have no surficial expression on the seafloor.

For the purposes of this report, an important issue is whether relief height influences megafaunal distribution and, if so, what is a suitable size category to separate low-relief from high-relief. Because of the high correlation between depth and relief, little new information was gained from correlations computed between taxonomic abundance and substrate size. The bivariate correlations between relief height and abundance, shown in Table 4, mirror the depth/abundance correlations shown in Table 3. The principal exception was the sea star of genus *Asterias*. This could explain its anomalous inclusion in Group A of primarily shallow taxa in Figure 3. During enumeration of color video images, it was clear that the largest boulders were unique biological habitats. Often they were covered with a high density of *M. senile* (frilled anemone). The following discussion seeks to determine whether this species or other taxa were included in the cluster groups of Figure 3, because of relief height rather than depth.

Stacked plots of depth, substrate size, and abundance for selected taxa are presented in Figures 6 through 11 for Transects 1 through 6, respectively. The depth profiles in the bottom frames of the figures show that five of the transects traversed both deep and shallow regions. The exception is Transect T1 (Figure 6) which traversed the comparatively shallow area atop the drumlin immediately north of the diffuser-cap corridor (Figure 1). Comparison substrate size, shown in the frame immediately above depth in Figures 6 through 11 and in depth profiles (bottom frame), corroborates their negative correlation. When water depth was shallow (<30 m), such as in Figure 6, the substrate tended to consist of rock, boulders, or even large boulders (unlabeled tick mark above “boulders”) with little cobble or deep sediments (tick mark labeled “none”). Transect T5 (Figure 10) provides another good example of this covariance where the shallow portion of the transect (Subsections S1 through S15) was the only region where substrate size exceeded that of cobbles.

Note that some transect subsections were much shorter than others, chiefly, for example, along Transect T1 (Figure 6, Subsections S6, S11, and S14) and Transect T6 (Figure 11, Subsections S10, S14, and S19). These short subsections contained isolated large boulders with a dimension exceeding 3 m (see size categories in Table 1). These very high relief substrates provided a habitat that was different from surrounding substrates, even boulders and large rocks. Shortening the 50-m nominal subsection length to include only these large boulders enabled computation of more accurate abundance estimates.

The extent to which the habitat differed on these and other hard-substrate features can be derived from the abundance of six selected taxa plotted in the upper frames of Figures 6 through 11. The *Asterias* spp. (sea star) taxon was selected because of its anomalous positive correlation with both depth and substrate relief. The taxa *P. magellanicus* (deep sea scallop) and *C. borealis* (northern cerianthid anemone) were representative of deep low-relief features as reflected in statistically-significant correlations shown in Tables 3 and 4. In contrast, the three remaining taxa typified shallow high-relief substrates. Of these three taxa, the distribution of *M. senile* (frilled anemone) abundance was particularly useful for distinguishing the influence of water depth from substrate relief. The only subsections where the lineal density of these organisms exceeded 10 m^{-1} , were those with large boulders. This supports anecdotal observations made during enumeration from color video concerning the tendency for this species to populate very high-relief substrates. However, some large boulders did not support an elevated abundance of this species. Along Transect T4 (Figure 9), the ROV encountered a large boulder at Subsection S13 that lacked a significant cover of *M. senile* (frilled anemone). This large boulder was the only one that also had a high ($>1 \text{ m}^{-1}$) abundance of *A. cribrosum* (sea colander) suggesting some competitive relationship between macroalgae and *Metridium* spp. Nevertheless, the uniqueness of the large boulder as a high-relief habitat is undeniable and these features are emphasized in recommended future sampling sites of Section 4.1.

Table 4. Pearson correlation coefficients between logarithmically-transformed taxon abundance and substrate size. Shaded coefficients are not statistically significant at the 95% confidence level.

Taxon	Common Name	Size Correlation
<i>Tautoglabrus adspersus</i>	cunner	0.55
<i>Metridium senile</i>	frilled anemone	0.51
<i>Rhodomenia palmata</i>	dulse	0.44
<i>Gadus morhua</i>	Atlantic cod	0.42
<i>Strongylocentrotus droebachiensis</i>	green sea urchin	0.36
<i>Boltenia ovifera</i>	stalked tunicate	0.34
<i>Agarum cribrosum</i>	sea colander	0.31
<i>Ciona intestinalis</i>	sea vase	0.30
<i>Rhodomenia</i> sp. A.	pinnate red algae	0.27
<i>Henricia sanguinolenta</i>	blood sea star	0.21
<i>Asterias</i> spp.	sea star	0.15
<i>Halocynthia pyriformis</i>	sea peach	0.14
<i>Porifera</i> sp. B.	leaf sponge	0.14
<i>Halichondria panicea</i>	crumb-of-bread sponge	0.12
<i>Henricia sanguinolenta</i> (juv)	blood sea star juvenile	0.09
<i>Modiolus modiolus</i>	northern horse mussel	0.09
<i>Balanus</i> spp.	barnacle	0.08
<i>Hemipterus americanus</i>	sea raven	0.00
<i>Clupea harengus</i>	Atlantic herring	0.00
<i>Crossaster papposus</i>	spiny sunstar	-0.01
<i>Psolus fabricii</i>	scarlet psolus	-0.05
<i>Haliclona oculata</i>	finger sponge	-0.06
<i>Homarus americanus</i>	American lobster	-0.06
<i>Porifera</i> spp.	sponge	-0.08
<i>Raja laevis</i>	barn-door skate	-0.08
<i>Melanogrammus aeglefinus</i>	haddock	-0.08
<i>Macrozoarces americanus</i>	ocean pout	-0.09
<i>Raja erinacea</i>	little skate	-0.10
<i>Pagurus</i> spp.	hermit crab	-0.11
<i>Urophycis</i> spp.	hake	-0.16
<i>Cerianthus borealis</i>	northern cerianthid	-0.20
<i>Myoxocephalus</i> spp.	sculpin	-0.21
<i>Cancer</i> spp.	crab	-0.23
<i>Pleuronectes americanus</i>	winter flounder	-0.24
<i>Placopecten magellanicus</i>	deep sea scallop	-0.26

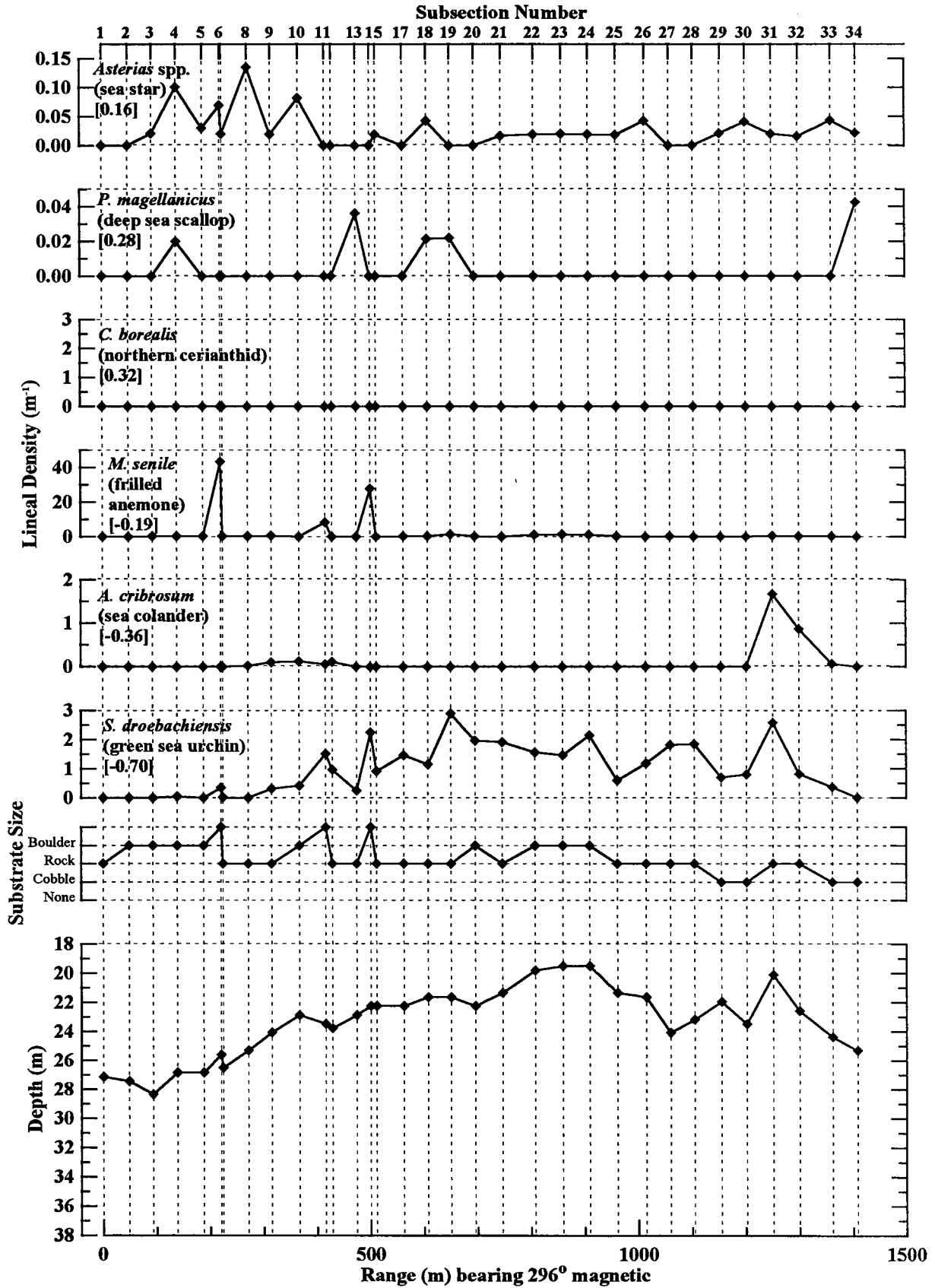


Figure 6. Variation in depth, substrate size and the abundance of six selected taxa along Transect T1.

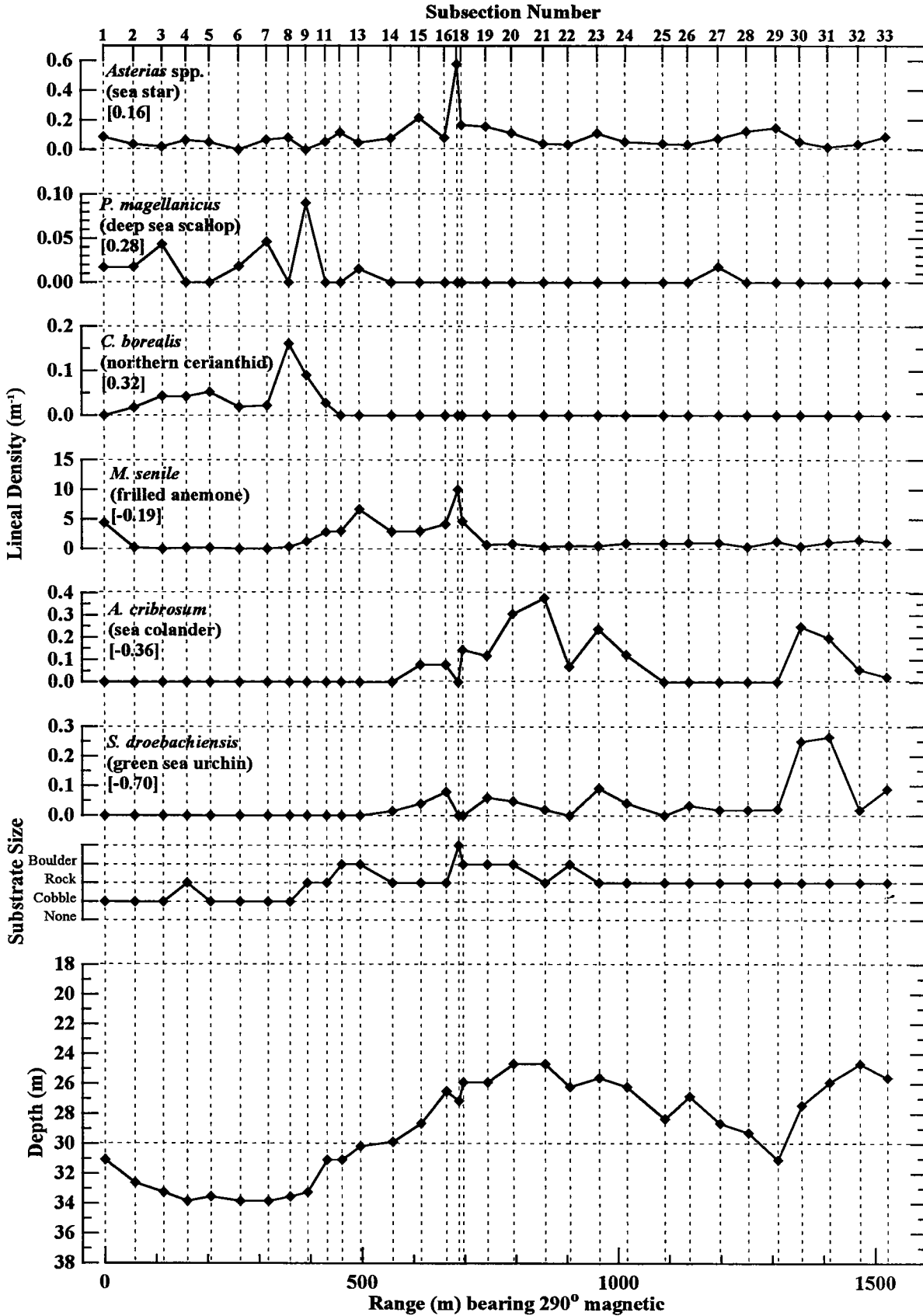


Figure 7. Variation in depth, substrate size and the abundance of six selected taxa along Transect T2.

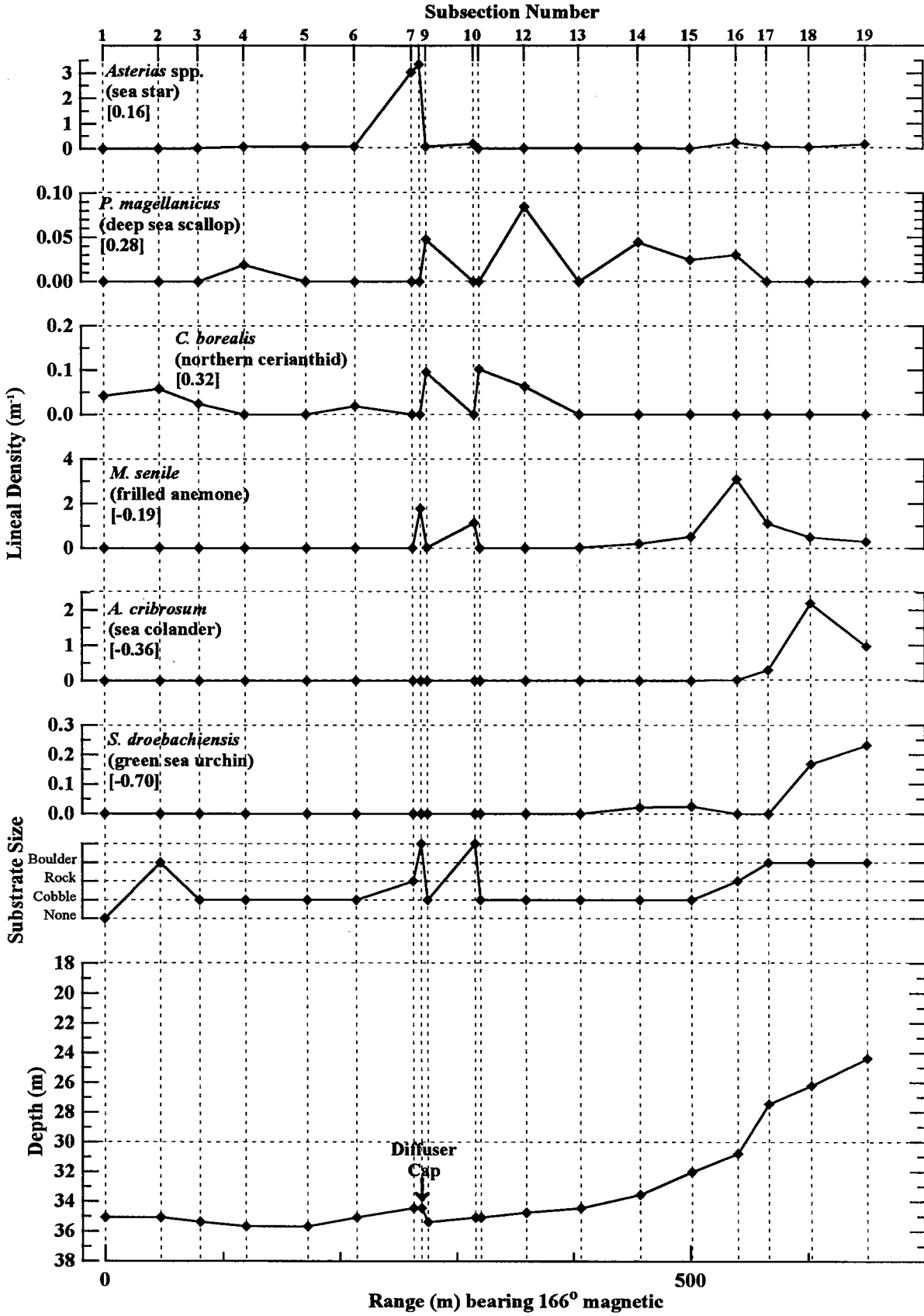


Figure 8. Variation in depth, substrate size and the abundance of six selected taxa along Transect T3.

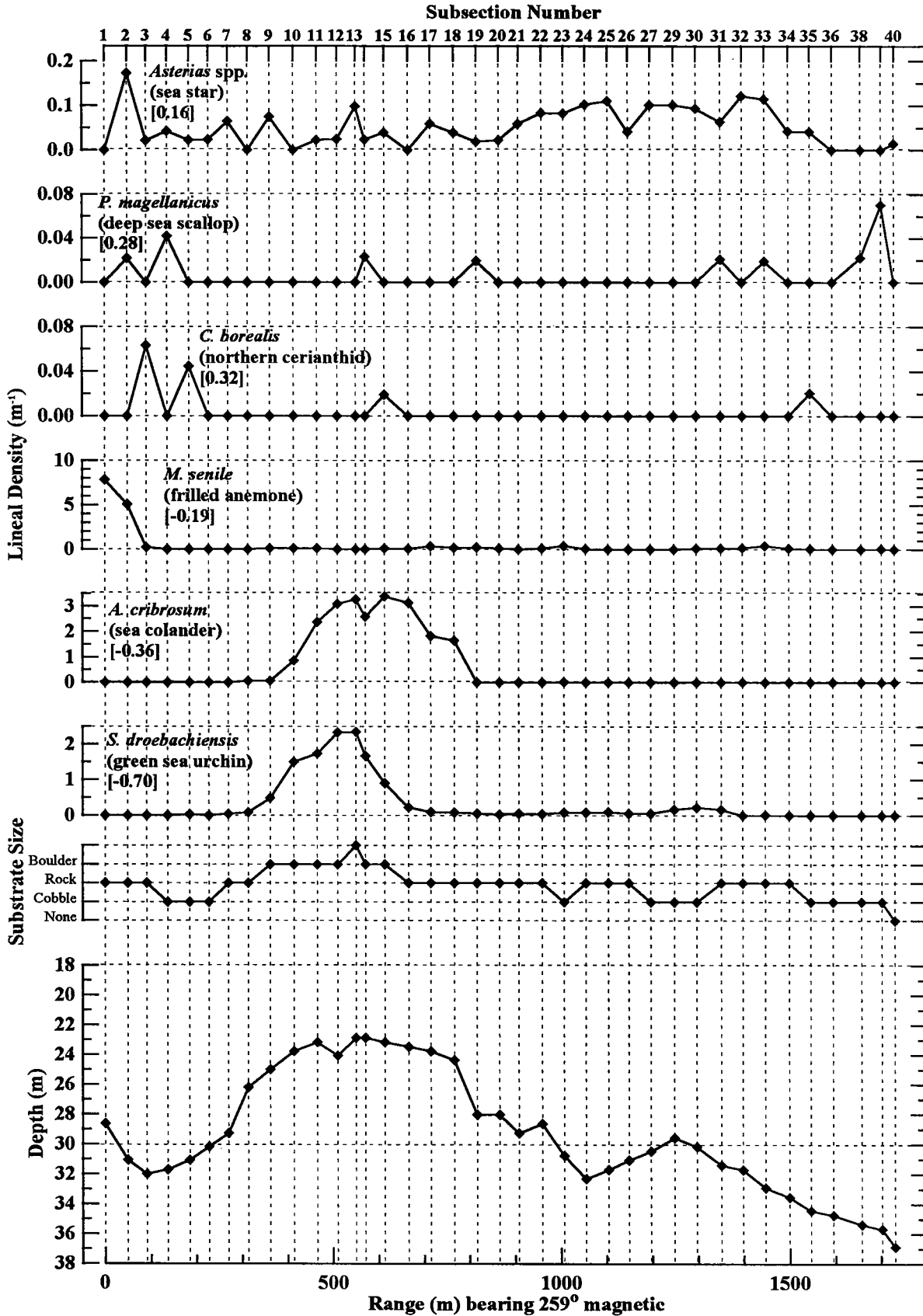


Figure 9. Variation in depth, substrate size and the abundance of six selected taxa along Transect T4.

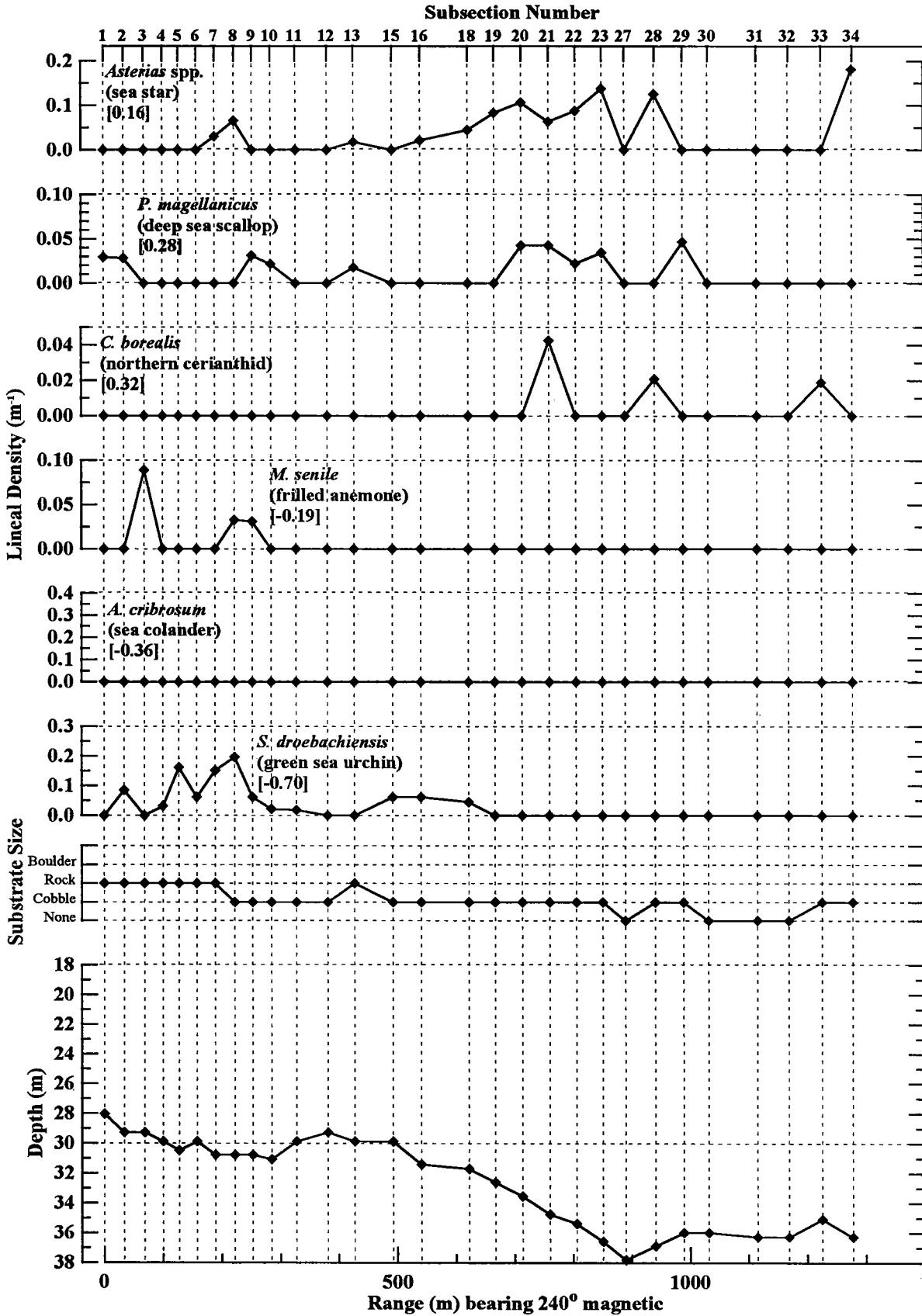


Figure 10. Variation in depth, substrate size and the abundance of six selected taxa along Transect T5.

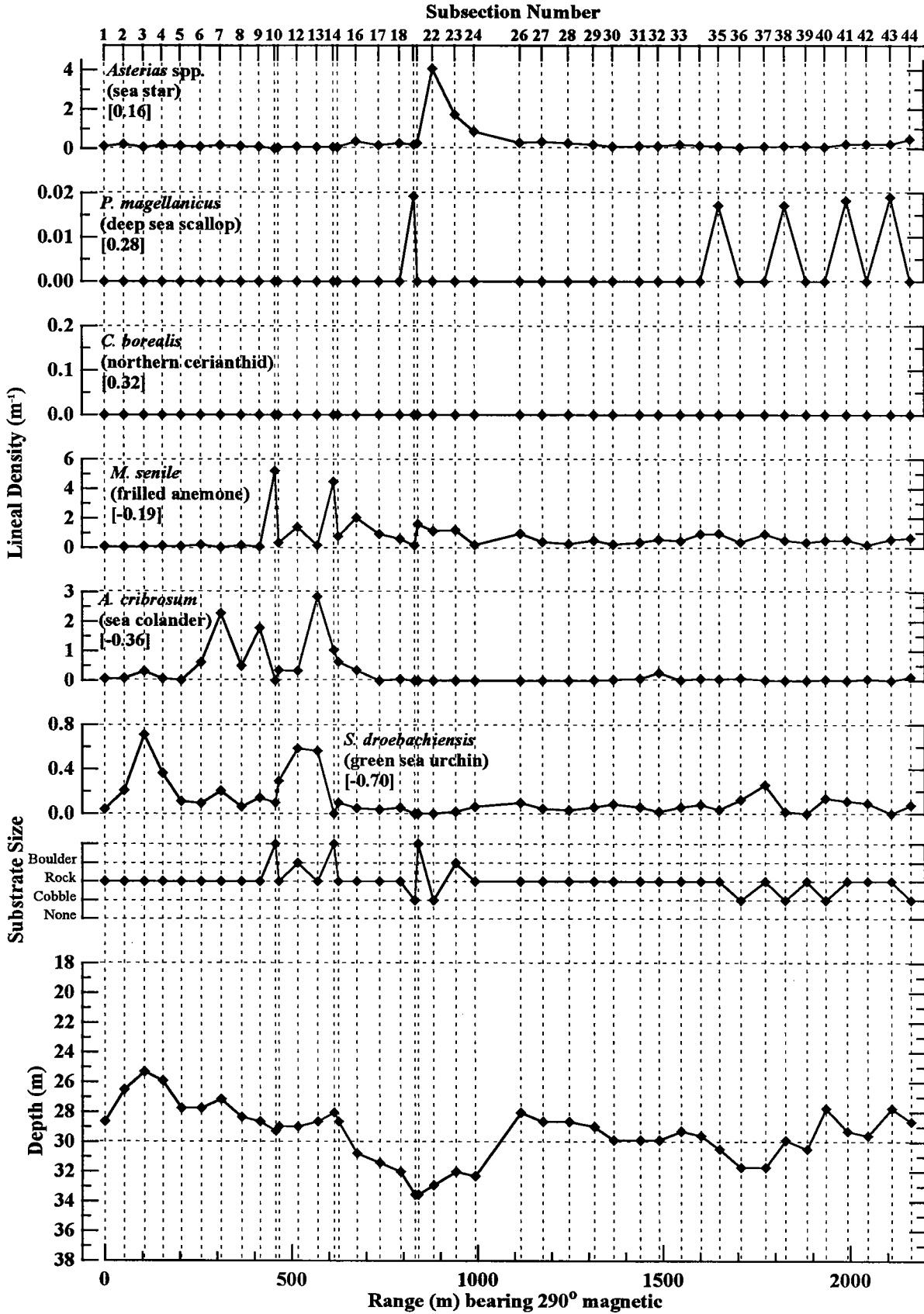


Figure 11. Variation in depth, substrate size and the abundance of six selected taxa along Transect T6.

The two taxa associated with deep water differed in their respective distributions. This lends further insight into relief height as a controlling factor. Anecdotal observations indicated that *C. borealis* (northern cerianthid anemone) was located within broad patches of sediment. These patches were often contained within cobbled subsections at depth. In contrast, *P. magellanicus* (deep sea scallop) was scattered among hard-substrate features and not always associated with deep sedimentary deposits. These observations are supported by Figures 6 through 11. *C. borealis* (northern cerianthid anemone) was almost absent at depths shallower than 30 m, and because of this, it achieved the highest positive depth correlation of any taxon (Table 3 and Figure 5). Elevated abundances of *P. magellanicus* (deep sea scallop) were, on the other hand, occasionally associated with shallower substrates of low relief (cobbles and rocks, cf. Figure 6). As a consequence, it exhibited the largest negative correlation with substrate size of any taxon (Table 4). Obviously, hard-substrate sites monitored in the future would exclude *C. borealis* (northern cerianthid anemone) in favor of *P. magellanicus* (deep sea scallop). However, both taxa were rare and any future monitoring program would probably undersample these species. Thus, exclusion of deep-sediment habitats and by association, *C. borealis* (northern cerianthid anemone), would not be detrimental to monitoring goals.

The distribution of *S. droebachiensis* (green sea urchin) closely tracks the depth profiles in Figures 6 through 11. This close correspondence explains why it had the largest negative correlation with depth, by far (Table 4). Its relationship to relief height was only weakly positive (Table 4). The depth dependence of the herbivore *S. droebachiensis* may be a consequence of the distribution of its food supply as reflected by the negative depth correlations in some algal taxa. The distribution of sea stars of the genus *Asterias* differed from that of other taxa because they were positively correlated with both water depth and substrate size. Because of the regional geomorphology described above, there were very few instances of deep high-relief features which makes the anomalous correlations even more curious. However, the anomalous correlations are the result of high *Asterias* spp. abundance ($>3 \text{ m}^{-1}$) near the diffuser cap surveyed on Subsection S8 of Transect 3 (Figure 8). The diffuser cap was one of the few very high relief features at depth. The large community of *Asterias* spp. on the cap may represent a transitional taxon on a substrate only recently introduced into the environment. The only other very high relief substrate at great depth was near the diffuser cap at Subsection S10. The population of *Asterias* spp. on that large boulder was much smaller (Figure 8).

The forgoing discussion described the importance of relief height, independent of water depth, in determining the distribution of some taxa. Thus, as in past studies, relief height should be included with water depth as a physical factor in tests for anthropogenic change. The distribution of *M. senile* (frilled anemone) in Figures 6 through 11 emphasizes the differences in boulder versus rock habitats. Thus, from Table 1, a reasonable transition diameter for distinguishing between high relief and low relief is 1 m. On the U.S. Pacific coast, Hardin *et al.* (1994) also defined high-relief as those hard-substrate features extending 1 m above the bottom.

3.2.3 Geographic Distribution

Given that water depth and substrate size are physical factors of interest, the task is now to specify transect subsections most representative of the four categories, deep high-relief, deep low-relief, shallow high-relief, and shallow low-relief. Again, the megafaunal community structure is used to define contiguous subsections where the substrate is typified by one of the four physical-factor categories and across-which megafaunal distributions are consistent. To aid in the selection of future hard-substrate monitoring sites, a dendrogram resulting from a numerical classification among transect subsections (Q mode) is presented in Figure 12. As expected, the highest Bray-Curtis similarities were often between adjacent subsections. Ten cluster groups were formed by contiguous subsections having high similarity.

For example, two cluster groups (T6-A and T6-B) formed along Transect T6 with respective Bray-Curtis similarities exceeding 0.78 and 0.70. Cluster Group T6-A includes Subsections S1 through S14 which were characterized by boulders and large rocks. These Subsections extended 625 m along the southeast portion of

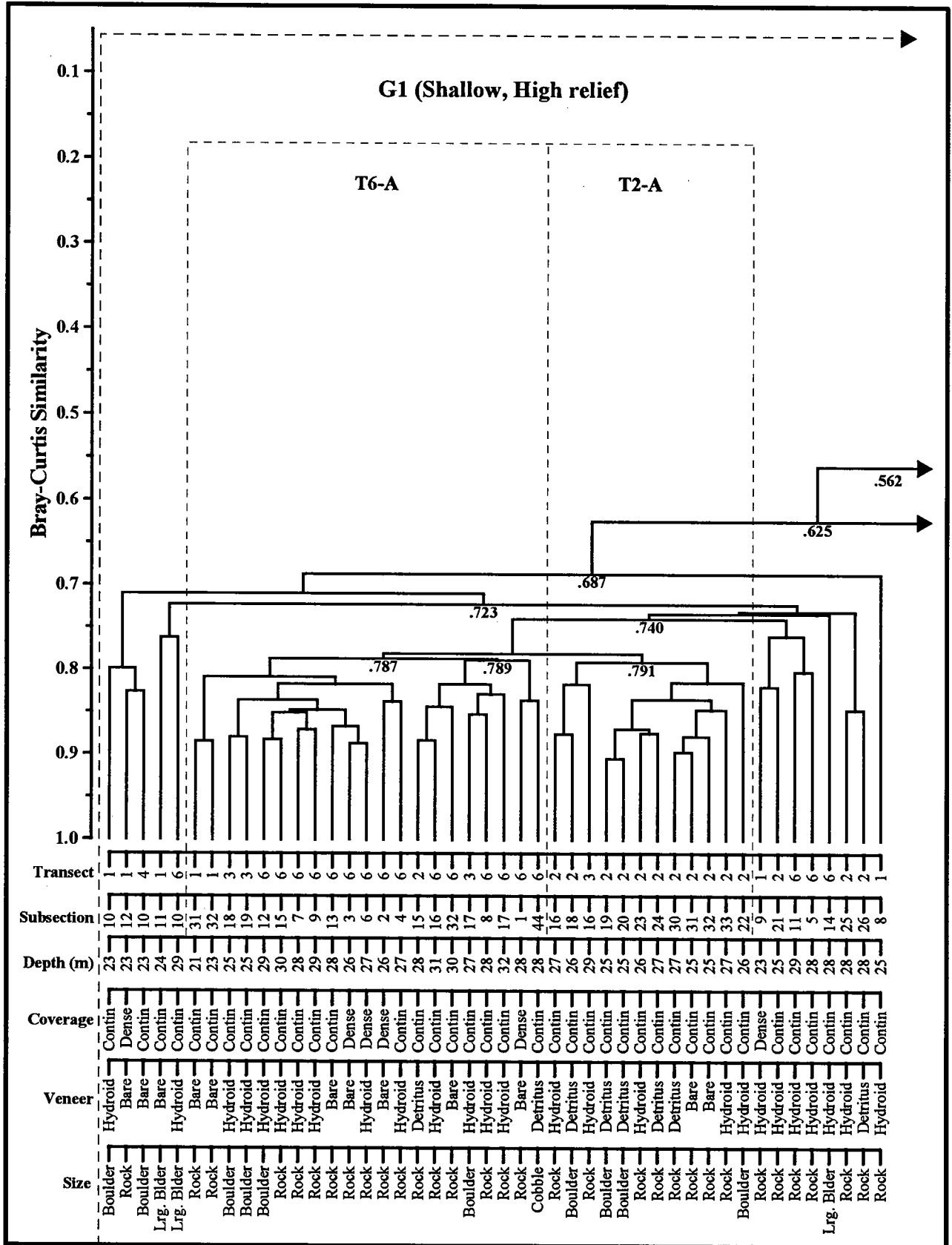


Figure 12. Dendrogram resulting from clustering (group average sorting) of Bray-Curtis similarity among transect subsections.

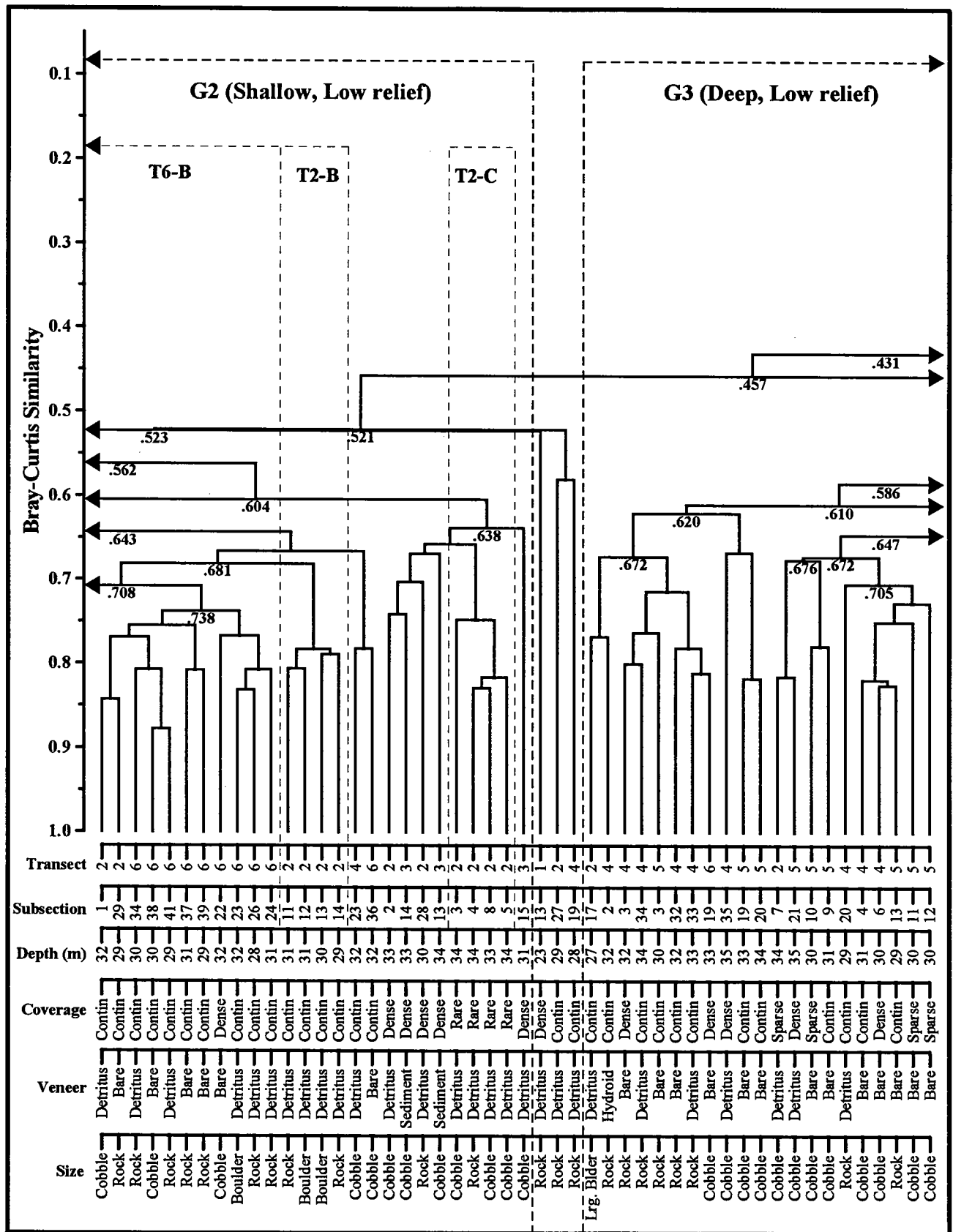


Figure 12 (continued). Dendrogram resulting from clustering (group average sorting) of Bray-Curtis similarity among transect subsections.

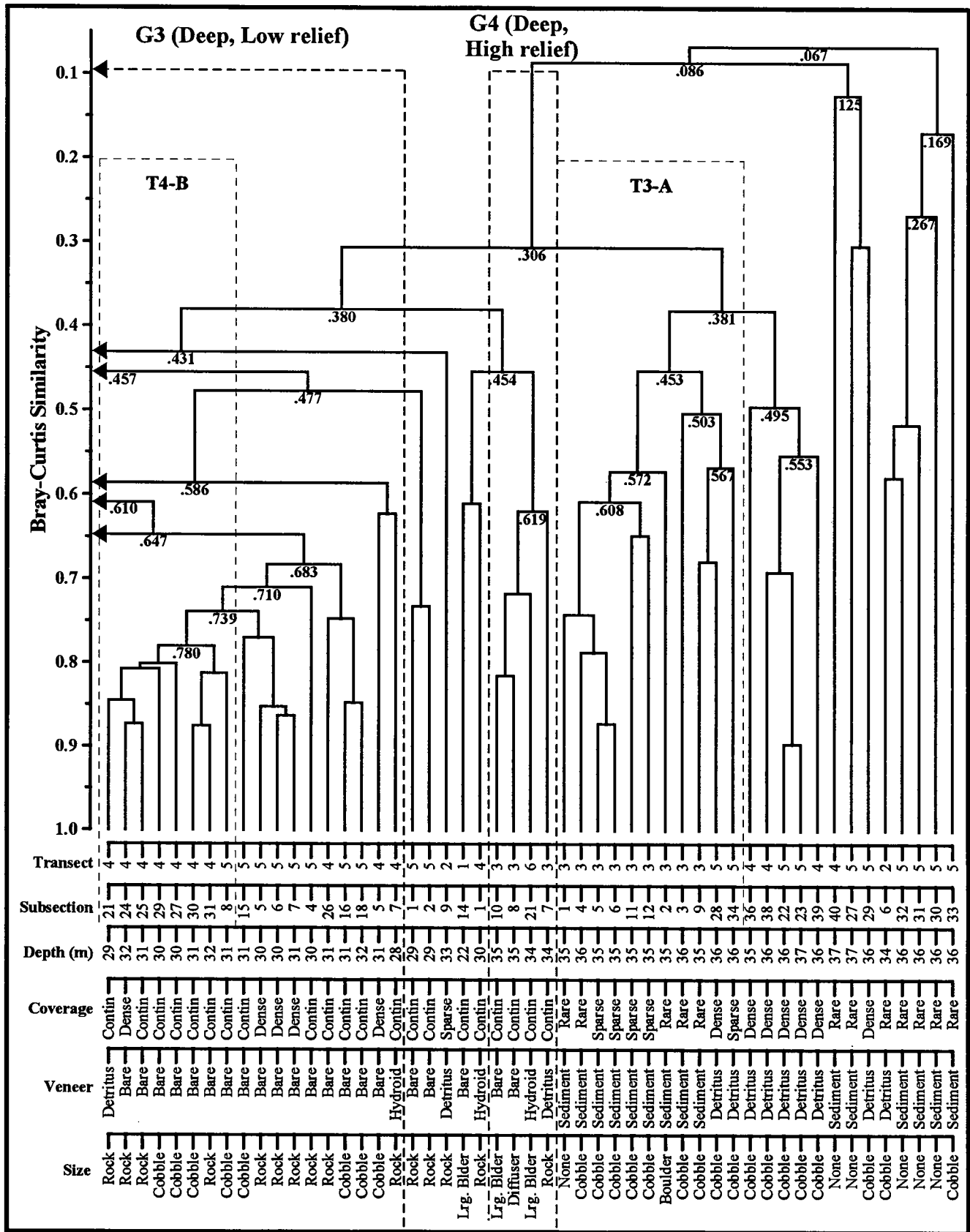


Figure 12 (continued). Dendrogram resulting from clustering (group average sorting) of Bray-Curtis similarity among transect subsections.

the Transect T6 which lies atop the drumlin immediately to the south of the diffuser cap corridor (Figure 1). In contrast, Cluster Group T6-B contained shallow low-relief features such as cobbles and small rocks (Figure 12). It included most Subsections between S25 and S45, and extended nearly 1 km along the northwest portion of T6. Analogous areas of contiguous subsections along other Transects clustered with high similarity as shown in Figure 12. At lower Bray-Curtis similarity, specifically a decision rule near $B=0.6$, these contiguous subsections formed cluster groups representative of the four combinations of physical factors. These are also indicated in Figure 12 as Major Cluster Groups G1 through G4.

Major Cluster Group G4 consisted of comparatively few transect subsections. This was a consequence of the paucity of deep high-relief features due to the regional geomorphology described previously. Indeed, one of the few deep high-relief features was artificially introduced into the deep environment. Diffuser cap number 23 was surveyed in Subsection S8 along Transect T3. Despite its relatively recent introduction, its megafaunal community clustered with that of other deep large boulders (Figure 12).

One cluster group (T3-A) of contiguous subsections along Transect T3, did not correspond to any of the major cluster groups. This cluster group covered Subsections S1 through S6 of Transect T3, which extended over deep sediments immediately north of the diffuser-cap corridor (Figure 1). Similarly, the megafaunal community within other subsections comprised mostly of deep sediments, did not compare with any of the four major cluster groups. These subsections exhibited the lowest similarity indices and are shown adjacent to Cluster Group T3-A at the end of the dendrogram. None are viable locations for hard-substrate sampling, but were included to investigate the character of existing (viz. Station S4) and potential infaunal sampling locations.

4.0 RECOMMENDATIONS

4.1 HARD-SUBSTRATE SITES

Sites recommended for future quantitative analyses of hard-substrate epifaunal communities are listed in Table 5. They are sorted by the four combinations of physical factors and list contiguous subsections indicative of similar megafaunal community structure as determined from Figure 12. Where applicable, cluster groups from Figure 12 are also indicated. The locations of the recommended sampling regions relative to the diffuser-cap corridor are shown in Figures 13 through 16 for each of the four combinations of physical factors. All contain sites that are both distant (>500 m) and close to the diffuser-cap corridor.

The recommended sampling sites do not include all possible sampling sites but were limited by the selection criteria described at the outset of this report. Other sites, potentially suitable for hard-substrate sampling, can be derived from the megafaunal database presented in the data report (Coats and Campbell, 1994). For example, the number and extent of deep high-relief sites (Figure 16) are limited compared to the sites representative of other combinations of physical factors. This group of recommended sites could be augmented by the isolated boulder located within the Subsection S2 of Transect T3 (*cf.*, Figure 8). During enumeration from video images, this boulder was not deemed of sufficient size to separate into a new subsection. Consequently, numerical classification indicated that the megafauna of this subsection was closely affiliated with other deep sedimentary sites within Cluster Group T3-A and not with the Major Cluster Group G4 indicative of high relief features (Figure 12). Other special cases also exist and additional analysis of the data may be warranted if the recommended sites are deemed insufficient or unsuitable.

4.2 NEAR-FIELD SEDIMENTARY SITES

Several regions of continuous sedimentary deposits of substantial extent were observed in the reconnaissance survey. These regions could potentially serve as soft-bottom sampling sites. One such region was successfully grab sampled at a site designated Station S4 in the soft-bottom benthic monitoring program of 1994 (Campbell, 1994). The broad extent of the sedimentary deposits without any indication of buried hard-substrate suggests that the deposits are deep and stable over time. Some are located in the extreme near-field, directly adjacent to the diffuser.

Three regions are particularly devoid of hard-substrate. The locations of these regions are listed in Table 6 and are shown in Figure 17. One set of contiguous subsections lies just north of the diffuser within a topographic low along Transect T3. Although these subsections include a single isolated boulder (Subsection S2 in Figure 8), they otherwise lack hard substrates. The estimated length of this sedimentary basin is listed as 175 m in Table 6, but it is likely that it covers a somewhat wider area. The region immediately north of Transect T3 was not surveyed but lies at a similar depth as the surveyed portion of the sedimentary basin. Similarly, Subsections S5 and S6 lie closer to the diffuser and were characterized by a sparse distribution of hard substrate. Thus, grab sampling may be possible at distances closer than 108 m (Table 6) to the diffuser caps as long as the rip-rap surrounding diffuser caps is avoided.

Table 5. Recommended hard-substrate sampling locations.

Substrate	Subsections	Cluster Group	First End Point	Second End Point	Length (m)	Mean Depth (m)	Closest Approach to Diffuser (m)
Shallow High Relief	T4(S8-S18)	T4-A	42° 23' 0.362" N 70° 47' 1.617" W	42° 22' 56.974" N 70° 47' 23.113" W	503	24	476
	T1(S1-S24)	T1-A	42° 23' 33.150" N 70° 48' 0.387" W	42° 23' 46.505" N 70° 48' 38.350" W	961	23	819
	T6(S1-S14)	T6-A	42° 22' 36.805" N 70° 46' 7.987" W	42° 22' 43.402" N 70° 46' 33.815" W	625	28	1168
	T3(S17-S20)		42° 23' 3.820" N 70° 47' 20.082" W	42° 22' 59.958" N 70° 47' 18.013" W	128	25	290
	T2(S15-S33)	T2-A	42° 23' 28.879" N 70° 47' 15.062" W	42° 23' 37.871" N 70° 47' 54.896" W	952	27	429
Shallow Low Relief	T1(S25-S35)	T1-B	42° 23' 46.505" N 70° 48' 38.350" W	42° 23' 53.271" N 70° 48' 57.942" W	494	24	1453
	T6(S26-S34)	T6-B	42° 22' 48.610" N 70° 46' 54.140" W	42° 22' 54.156" N 70° 47' 16.222" W	533	29	600
	T6(S38-S45)	T6-B	42° 22' 56.058" N 70° 47' 23.527" W	42° 22' 59.805" N 70° 47' 38.548" W	363	29	303
Deep Low Relief	T5(S4-S23)		42° 22' 47.793" N 70° 47' 2.820" W	42° 22' 34.416" N 70° 47' 31.788" W	781	32	868
	T4(S2-S6)		42° 23' 2.655" N 70° 46' 50.139" W	42° 23' 1.062" N 70° 46' 59.824" W	227	31	489
	T4(S23-S39)	T4-B	42° 22' 55.601" N 70° 47' 31.244" W	42° 22' 50.394" N 70° 48' 2.124" W	724	33	447
	T2(S1-S8)	T2-C	42° 23' 21.500" N 70° 46' 50.112" W	42° 23' 25.585" N 70° 47' 6.423" W	394	33	64
Deep High Relief	T6(S21-S25)		42° 22' 45.556" N 70° 46' 42.765" W	42° 22' 47.937" N 70° 46' 51.695" W	217	32	928
	T3(S8)	Diffuser	42° 23' 13.383" N 70° 47' 22.100" W	42° 23' 13.132" N 70° 47' 22.386" W	10	35	3
	T3(S10)		42° 23' 11.768" N 70° 47' 22.387" W	42° 23' 11.599" N 70° 47' 22.435" W	5	35	39
	T2(S12-S13)		42° 23' 25.577" N 70° 47' 9.462" W	42° 23' 27.107" N 70° 47' 13.398" W	102	30	298

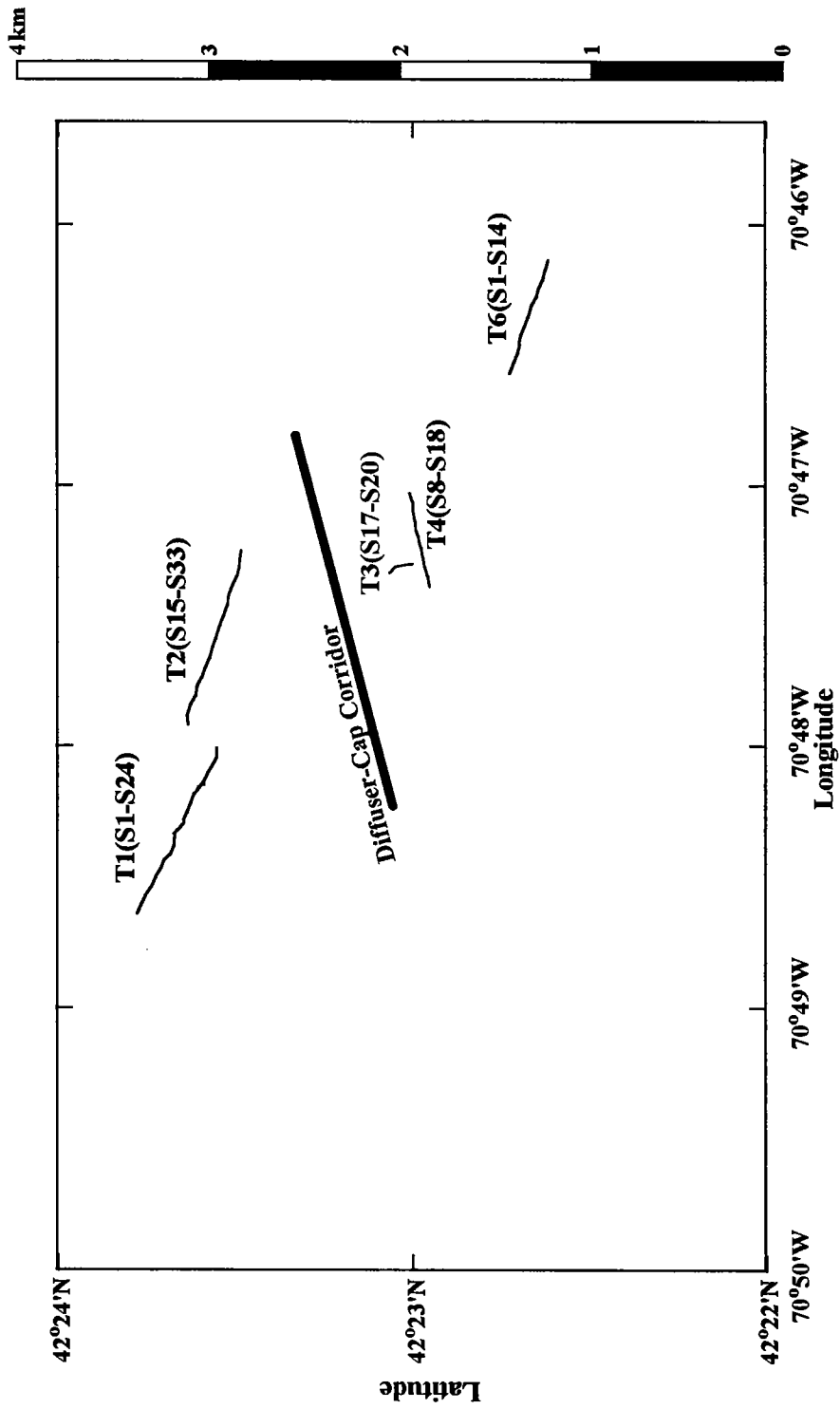


Figure 13. Location of shallow high-relief sites listed in Table 5. Numbers with a "T" prefix refer to transects and the "S" prefix indicates subsections.

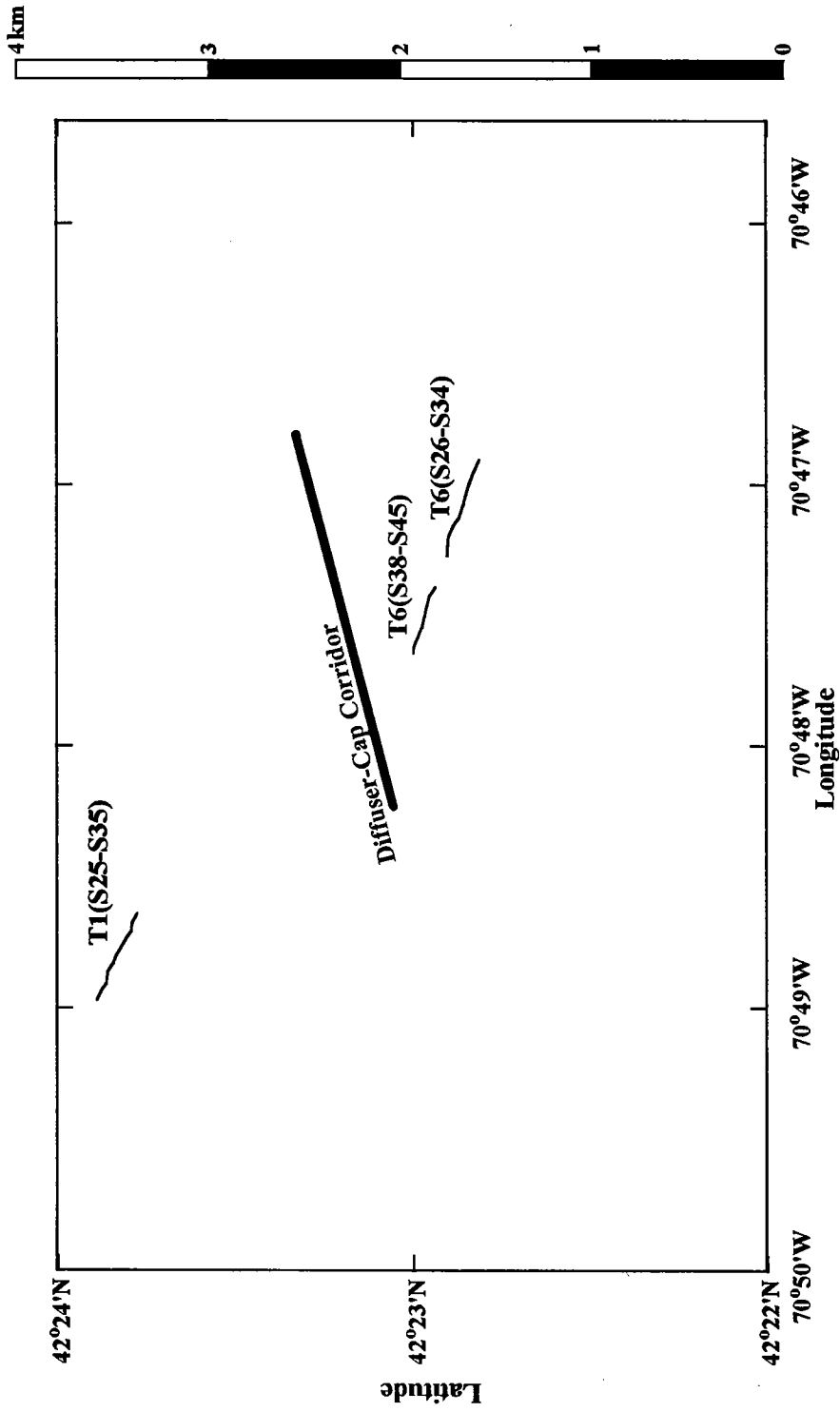


Figure 14. Location of shallow low-relief sites listed in Table 5. Numbers with a "T" prefix refer to transects and the "S" prefix indicates subsections.

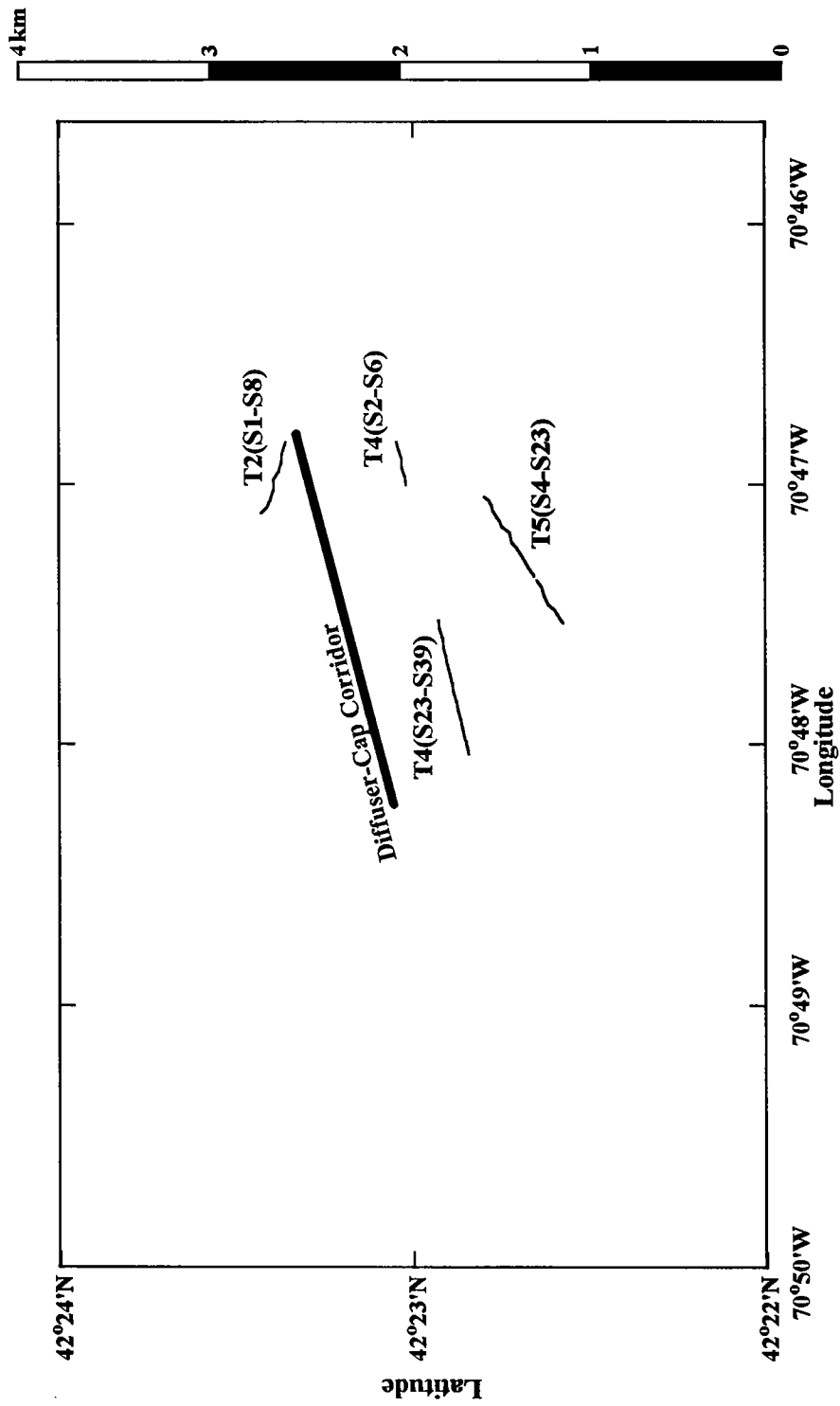


Figure 15. Location of deep low-relief sites listed in Table 5. Numbers with a "T" prefix refer to transects and the "S" prefix indicates subsections.

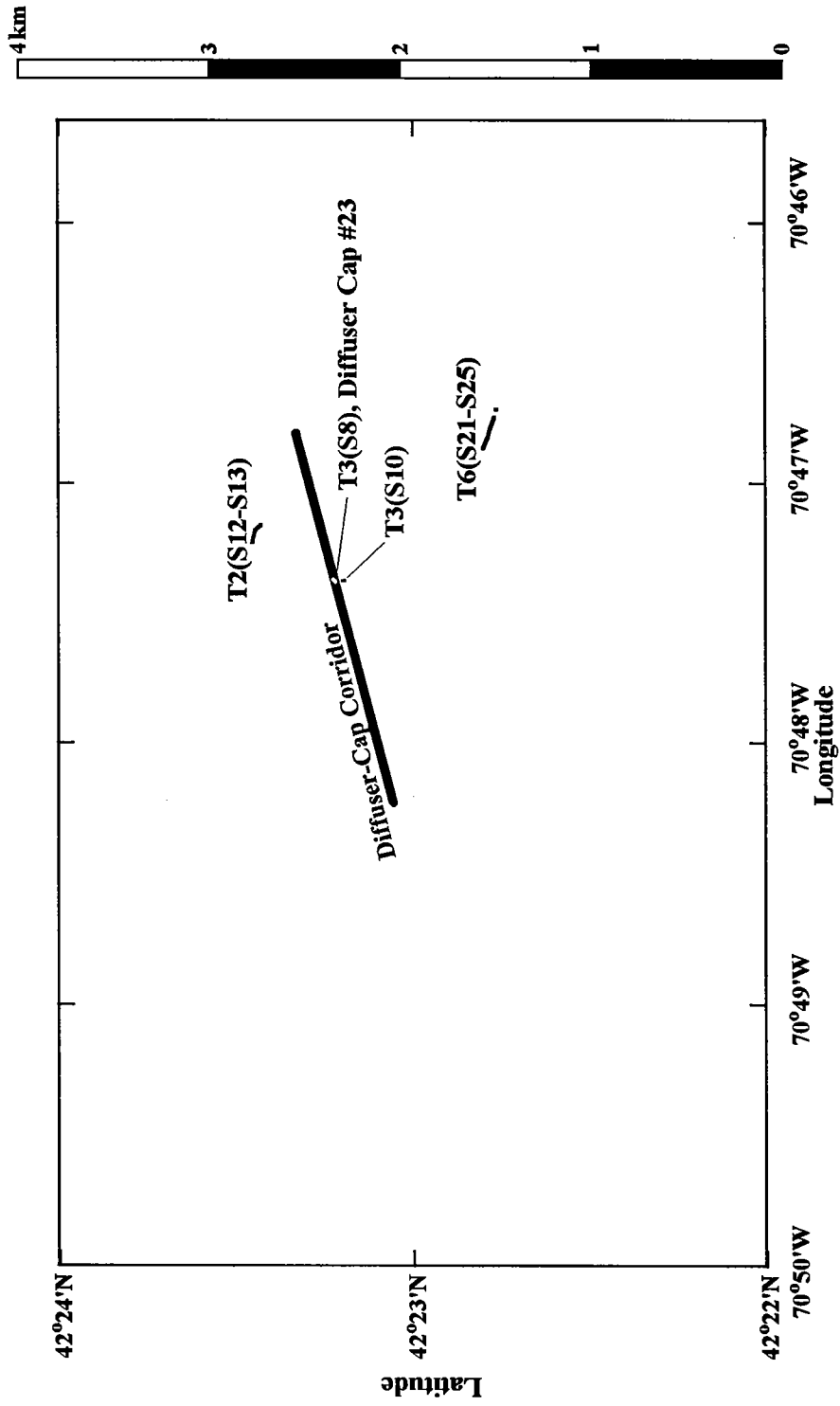


Figure 16. Location of deep high-relief sites listed in Table 5. Numbers with a "T" prefix refer to transects and the "S" prefix indicates subsections.

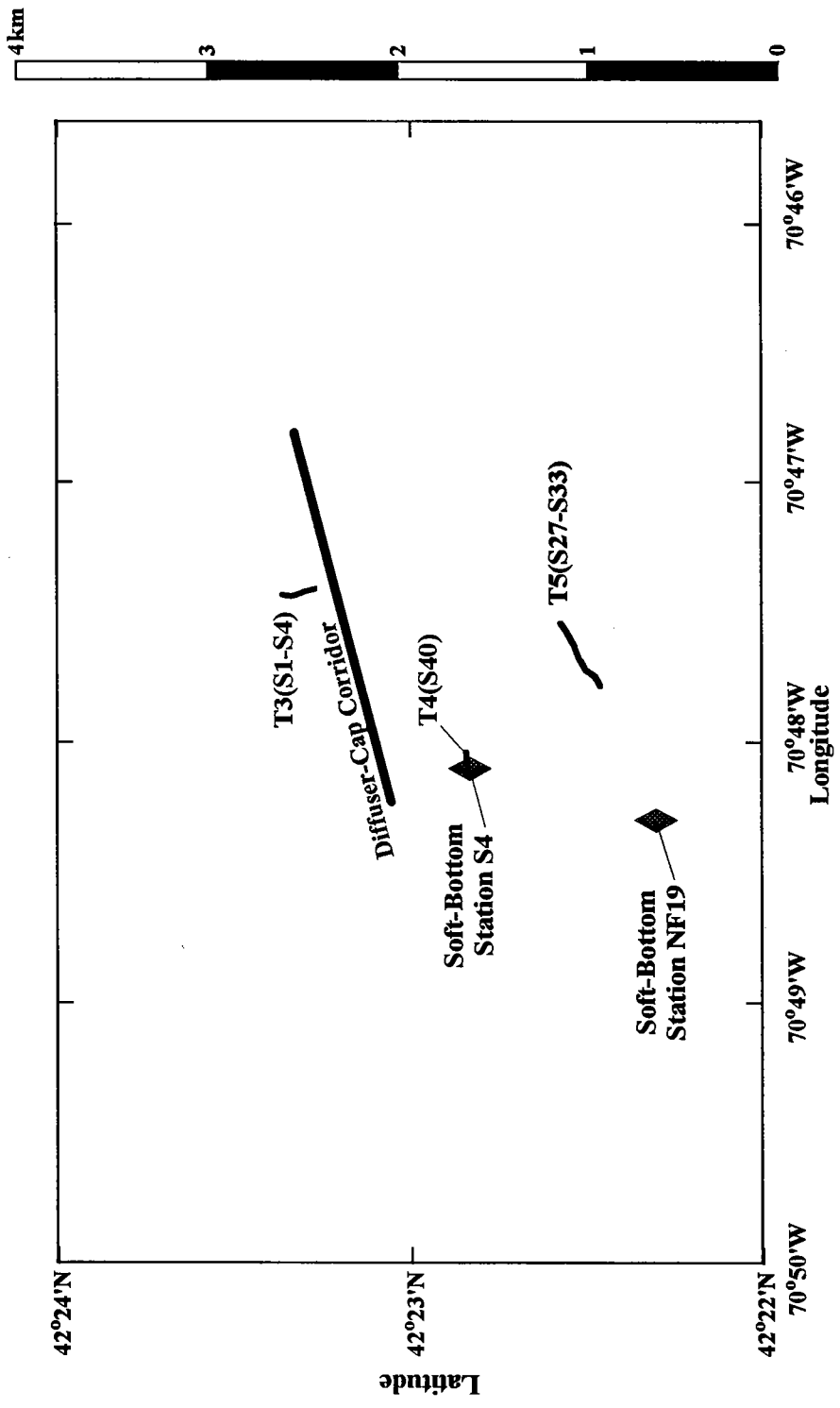


Figure 17. Location of deep sediment sites and the benthic infaunal sampling Stations S4 and NF19. Numbers with a "T" prefix refer to transects and the "S" prefix indicates subsections.

Table 6. Location of deep sedimentary deposits.

Subsections	First End Point	Second End Point	Length (m)	Mean Depth (m)	Closest Approach to Diffuser (m)
T3(S1-S4)	42° 23' 21.696" N 70° 47' 25.775" W	42° 23' 16.225" N 70° 47' 24.300" W	175	35	108
T4(S40)	42° 22' 50.394" N 70° 48' 2.124" W	42° 22' 50.072" N 70° 48' 5.007" W	67	37	447
T5(S27-S33)	42° 22' 34.242" N 70° 47' 32.156" W	42° 22' 27.535" N 70° 47' 46.518" W	303	36	1084

Another large area of deep sedimentary deposits was encountered along Transect T5, at Subsections S27 through S33. Again, the full lateral extent of the sediment is likely to be much larger than 303 m listed in Table 6. Indeed, these subsections lie at the end of the surveyed portion of Transect T5 where the planned ROV transit was stopped early specifically due to the lack of hard substrate (Figure 2). If the transect had continued, it would have passed close to the benthic infaunal Station NF19 (Figure 17) which has been successfully sampled in 1992 (Blake *et al.*, 1993) and in 1994 (Campbell, 1994). This suggests that the length of this sedimentary deposit extends beyond 1 km.

The other region of notable sedimentary deposits lies close to the benthic infaunal Station S4. Transect T4 was terminated at Station S4 so the lateral extent of sedimentary deposits is again indeterminate. However, Subsection S39, which lies immediately to the east of Subsection S40, was densely cobbled. This indicates that soft-bottom sampling near Station S4 is restricted to within approximately 67 m of its present location. The deep sediments of Subsection S40 supported an unusual megafaunal community, even among sedimentary deposits along other Transects. This difference is reflected in its low similarity index (0.125, near the end of Figure 12) and was due to a comparatively large population of *Urophycis* spp. (hake) residing in a complex of small burrows hollowed out of the fine-grained sediments.

5.0 LITERATURE CITED

- Auster, P.J., R.J. Malatesta, S.C. LaRosa, R.A. Cooper, and L.L. Stewart. 1991. **Microhabitat utilization by the megafaunal assemblage at a low relief outer continental shelf site - Middle Atlantic Bight, USA.** *J. Northwest Atl. Fish. Sci.* 11:59-69.
- Battelle Ocean Sciences Ocean Sciences Center. 1987. **Benthic Reconnaissance.** Final report prepared for Camp Dresser and McKee/Stone & Webster Engineering Corporation. Revised May 15, 1987. 70 pp.
- Blake, J.A., D.C. Rhoads, and B. Hilbig. 1993. **Massachusetts Bay outfall monitoring program: soft-bottom benthic biology and sedimentology, 1992 baseline conditions in Massachusetts and Cape Cod Bays.** MWRA Enviro. Quality Dept. Tech. Rpt. Series No. 93-10. Massachusetts Water Resources Authority, Boston, MA. 108 pp. + 4 appendices.
- Boesch, D.F. 1977. **Application of numerical classification in ecological investigations of water pollution.** Virginia Institute of Marine Science, Gloucester Point, VA. Environmental Research Laboratory, Office of Research and Development, U.S. Environmental Protection Agency. EPB-600/3-77-033. March. 114 pp.
- Bothner, M.H., C.M. Parmenter, D.C. Twichell, C.F. Polloni, and H.J. Knebel. 1992. **A geologic map of the sea floor in western Massachusetts Bay, constructed from digital sidescan sonar images, photography, and sediment samples.** U.S. Geological Survey Digital Data Series DDS-3, 1 CD-ROM.
- Campbell, J.F. 1994. **Nearfield/Farfield Survey S9403 Report for Soft-Bottom Benthic Monitoring: 1993-1994, Task 11.1 and 11.2.** MWRA Enviro. Quality Dept. Rpt. Massachusetts Water Resources Authority, Boston, MA. 13 pp.
- Clifford, H.T. and W. Stephenson. 1975. **An Introduction to Numerical Classification.** Academic Press, New York, NY. 229 pp.
- Coats, D.A. and J.F. Campbell. 1994. **Hard-Substrate Reconnaissance Survey S9404 Data Report for MWRA Harbor and Outfall Monitoring Project.** MWRA Enviro. Quality Dept. Rpt. Massachusetts Water Resources Authority, Boston, MA. 15 pp + 1 appendix.
- Coats, D.A., E. Imamura, and J.F. Campbell. 1995. **Draft Report: 1993 Annual Soft-Bottom Benthic Monitoring, Massachusetts Bay Outfall Studies.** MWRA Enviro. Quality Dept. Rpt. Massachusetts Water Resources Authority, Boston, MA. 115 pp.
- Davis, D.L. and C.H. Pilskaln. 1992. **Measurements with underwater video: camera field width calibration and structured lighting.** *Marine Technology Society Journal.* 26(4).
- Foster, M.S., C. Harrold, and D.D. Hardin. 1991. **Point vs. Photo Quadrat Estimates of the Cover of Sessile Marine Organisms.** *Journal of Experimental Marine Biology and Ecology,* 146:193-203.
- Hardin, D.D., D.A. Coats, J.F. Campbell and E. Imamura. 1993. **A Survey of Prominent Anchor Scars and the Level of Disturbance to Hard-Substrate Communities in the Point Arguello Region.** Submitted to Chevron USA, Inc., by Marine Research Specialists, October 1993. 55 pp.

- Hardin, D.D., J. Toal, T. Parr, P. Wilde, and K. Dorsey. 1994. **Spatial variation in hard-bottom epifauna in the Santa Maria Basin, California: the importance of physical factors.** *Marine Environmental Research*. Vol. 37(1994): 165-193.
- Haedrich, R.L., G.T. Rowe, and P.T. Polloni. 1975. **Zonation and faunal composition of epibenthic populations on the continental slope south of New England.** *Journal of Marine Research*. 33: 191-212.
- Hecker, B. 1990. **Variation in megafaunal assemblages on the continental margin south of New England.** *Deep-Sea Research*. 37A:37-57.
- Hyland, J., D. Hardin, M. Steinhauer, D. Coats, R. Green, and J. Neff. 1994. **Environmental Impact of Offshore Oil Development on the Outer Continental Shelf and Slope off Point Arguello, California.** *Marine Environmental Research*. Vol. 37(1994): 195-229.
- Imamura, E. 1994. **Hard-Bottom Reconnaissance Survey S9404 Report for Hard-Bottom Studies: 1993-1994, Subtask 20.1.** MWRA Enviro. Quality Dept. Tech. Rpt. Massachusetts Water Resources Authority, Boston, MA. 7 pp.
- Knebel, H.J. 1993. **Sedimentary environments within a glaciated estuarine-inner shelf system: Boston Harbor and Massachusetts Bay.** *Marine Geology*. 110:7-30.
- Michalopoulos, C., P.J. Auster, and R.J. Malatesta. 1992. **A Comparison of Transect and Species-Time Counts for Assessing Faunal Abundance from Video Surveys.** *Marine Technology Society Journal*. 26(4): 27-31.
- Rowe, G.T. and R.J. Menzies. 1969. **Zonation of large benthic invertebrates in the deep-sea off the Carolina.** *Deep-Sea Research*. 16:531-581.
- Sneath, P.H.A. and R.R. Sokal. 1973. **Numerical Taxonomy. The Principles and Practice of Numerical Classification.** W.H. Freeman and Co., San Francisco, CA. 573 pp.
- Swartz, R.C. 1978. **Techniques for sampling and analyzing the marine macrobenthos.** U.S. Department of Commerce National Technical Information Service. PB-35-281 631, Corvallis Environmental Research Laboratory, Corvallis, OR.
- Taylor, W.R. 1962. **Marine algae of the northeastern coast of North America.** Second ed., revised (1957), second printing corrected 1962. University of Michigan Press, Ann Arbor. 509 pp.
- Tusting, R.F. and D.L. Davis. 1992. **Laser Systems and Structured Illumination for Quantitative Undersea Imaging.** *Marine Technology Society Journal*. 26(4): 5-12.
- Uzmann, J.R., R.A. Cooper, R.B. Theroux, and R.L. Wigley. 1977. **Synoptic comparison of three sampling techniques for estimating abundance and distribution of selected megafauna: submersible vs camera sled vs otter trawl.** *Marine Fisheries Review*. 39:11-19.
- Wakefield, W.W. and A. Genin. 1987. **The use of a Canadian (perspective) grid in deep-sea photography.** *Deep-Sea Research*. 34: 469-478.

Witman, J.D. and K.P. Sebens. 1993. **Rocky subtidal communities in Massachusetts Bay: Lovell Island to Nahant Transect. A final report on the 1991 - 1992 sampling period.** MWRA Enviro. Quality Dept. Tech. Rpt. Series No. 93-13. Massachusetts Water Resources Authority, Boston, MA. 137 pp.



The Massachusetts Water Resources Authority
Charlestown Navy Yard
100 First Avenue
Charlestown, MA 02129
(617) 242-6000